

Synchrotron PXRD deconvolutes nickel particle and support changes in Ni/ZrO₂ methanation catalysts - ESI

Mariam L. Schulte,^{a,b,‡} Sebastian Weber,^{a,b,‡} Linda Klag,^a Jan-Dierk Grunwaldt^{a,b}
and Thomas L. Sheppard^{*a,b}

^a Institute for Chemical Technology and Polymer Chemistry, Karlsruhe Institute of Technology (KIT), Engesserstr. 20, 76131 Karlsruhe, Germany. Tel: +4972160847989; E-mail: thomas.sheppard@kit.edu

^b Institute of Catalysis Research and Technology, Karlsruhe Institute of Technology (KIT), Hermann-von-Helmholtz-Platz 1, 76344 Eggenstein-Leopoldshafen, Germany.

‡ These authors contributed equally.

Contents

1	Laboratory characterization	3
2	Laboratory catalytic testing	12
3	<i>Operando</i> SPXRD experiments	15
4	Rietveld refinements of the laboratory PXRD and SPXRD experiments	21

1 Laboratory characterization

Table S 1 Summary of the laboratory characterization results for the different ZrO_2 supports of the study before Ni deposition, with Z25 as supplied.

supports	$A_{\text{BET}} / \text{m}^2 \text{ g}^{-1}$	$V_p / \text{cm}^3 \text{ g}^{-1}$	$L_{\text{vol}}(\text{ZrO}_2) / \text{nm}$
Z25	100	0.24	9.5
Z350	93	0.23	9.5
Z500	51	0.19	13
Z650	26	0.043	23
Z800	13	0.021	41
Z1000	5	0.009	116

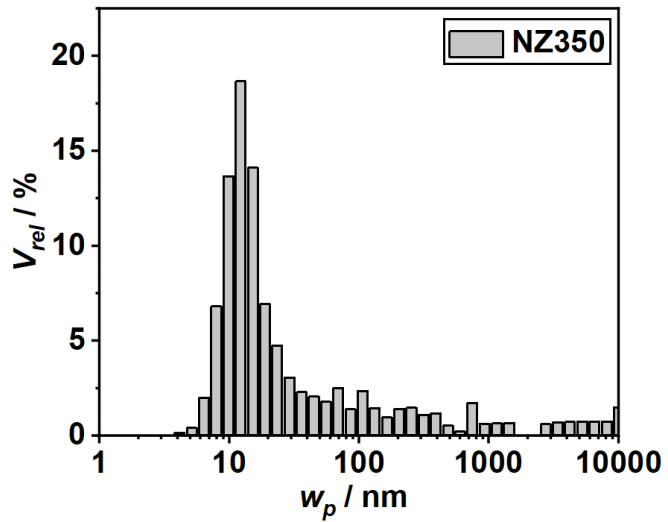


Figure S 1 Pore width distribution w_p obtained by MIP for NZ350 catalyst.

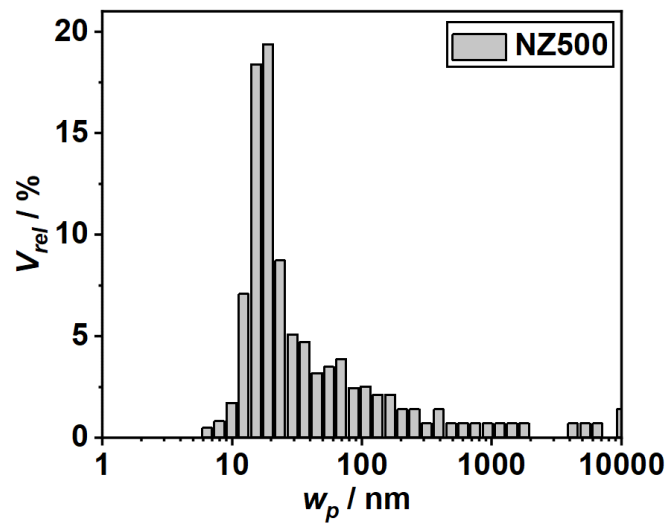


Figure S 2 Pore width distribution w_P obtained by MIP for NZ500 catalyst.

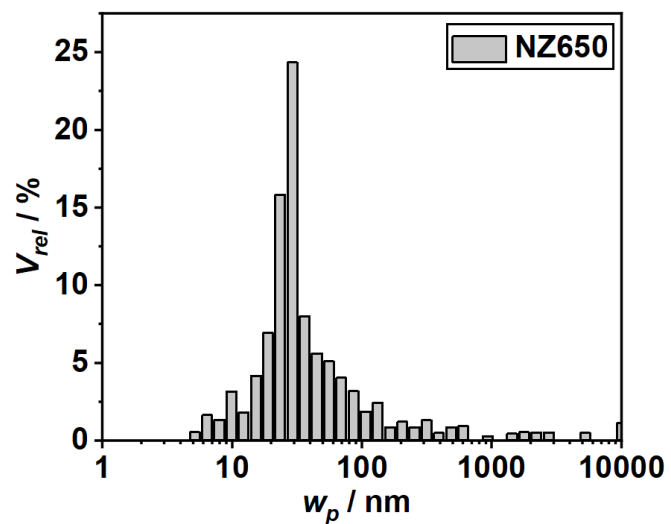


Figure S 3 Pore width distribution w_P obtained by MIP for NZ650 catalyst.

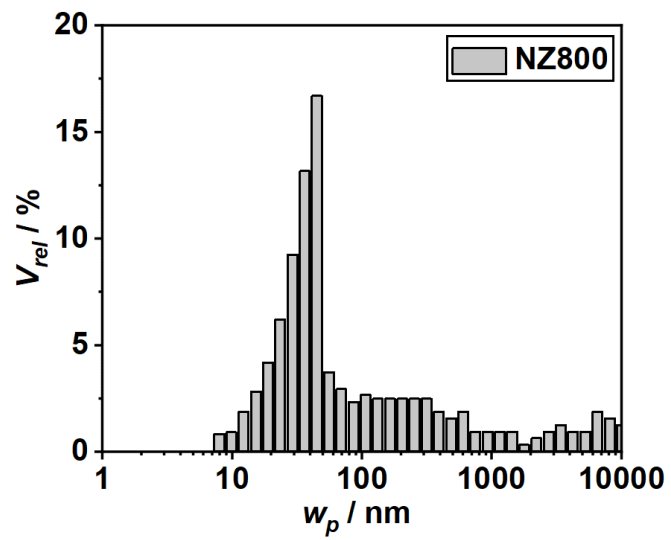


Figure S 4 Pore width distribution w_p obtained by MIP for NZ800 catalyst.

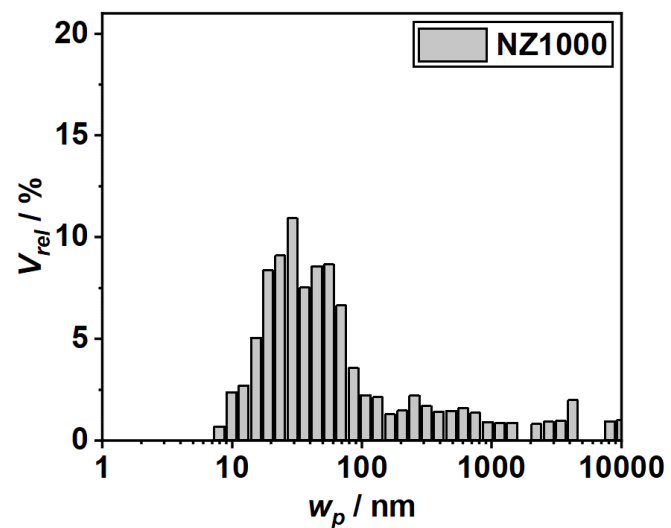


Figure S 5 Pore width distribution w_p obtained by MIP for NZ1000 catalyst.

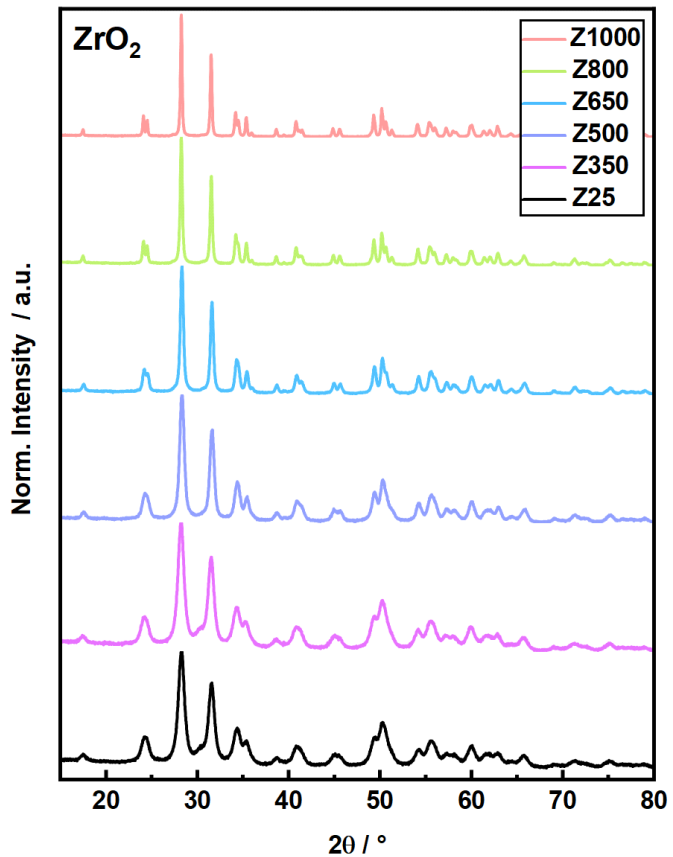


Figure S 6 XRD patterns of the pure ZrO_2 support prior calcination (Z25) and calcined at temperatures between 523 K and 1273 K (Z350-Z1000). All samples show mainly the presence of m- ZrO_2 , while Z25 and Z350 show small contributions of t- ZrO_2 as shown in Figure S 7 and Table S 2.

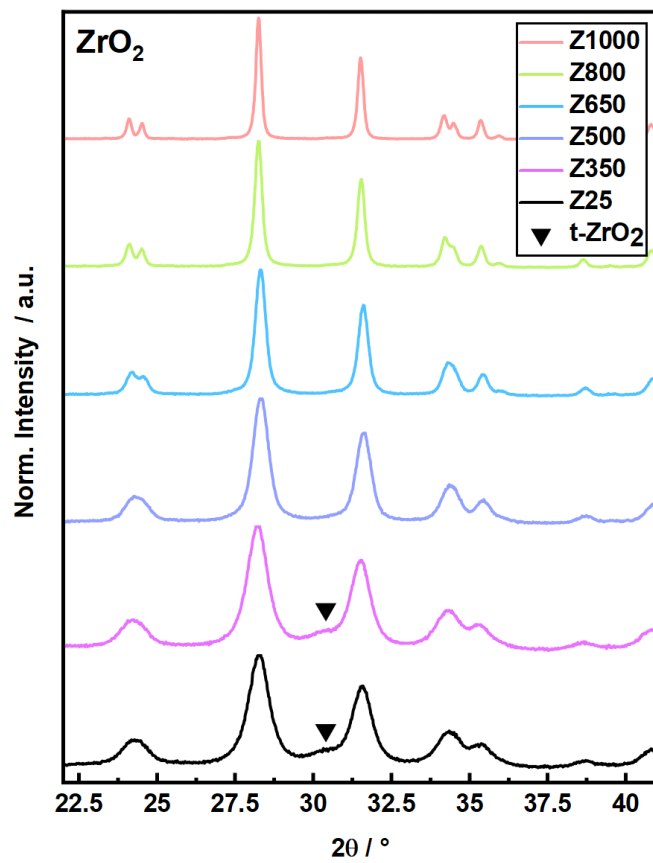


Figure S 7 Zoomed XRD patterns of Figure S 6 for the pure ZrO_2 support prior calcination (Z25) and calcined at temperatures between 523 K and 1273 K (Z350-Z1000). The features marked with black triangle can be assigned to t- ZrO_2 .

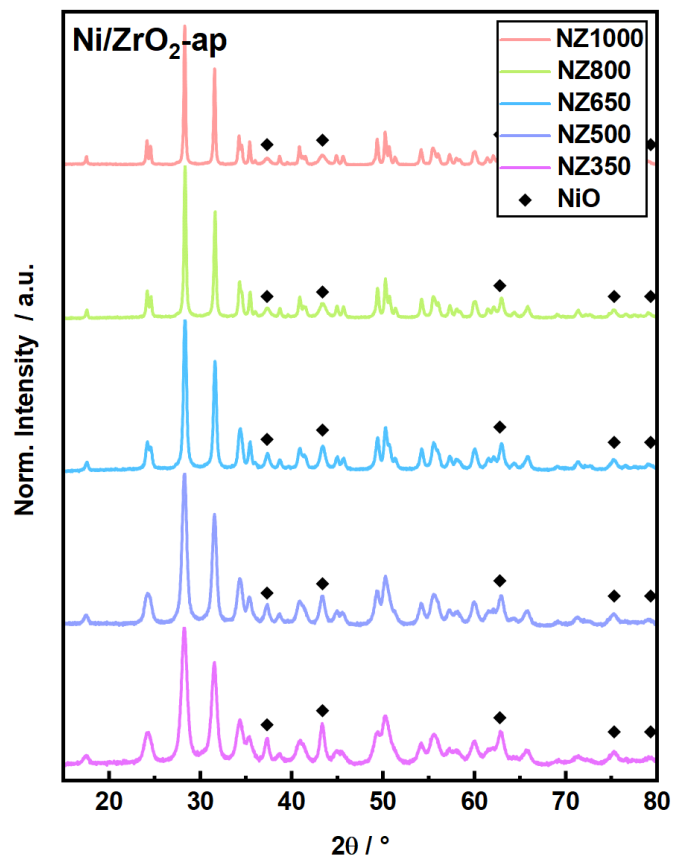


Figure S 8 XRD patterns of as-prepared Ni/ZrO₂ catalysts (NZ350-NZ1000). The present NiO is marked with black rhombus.

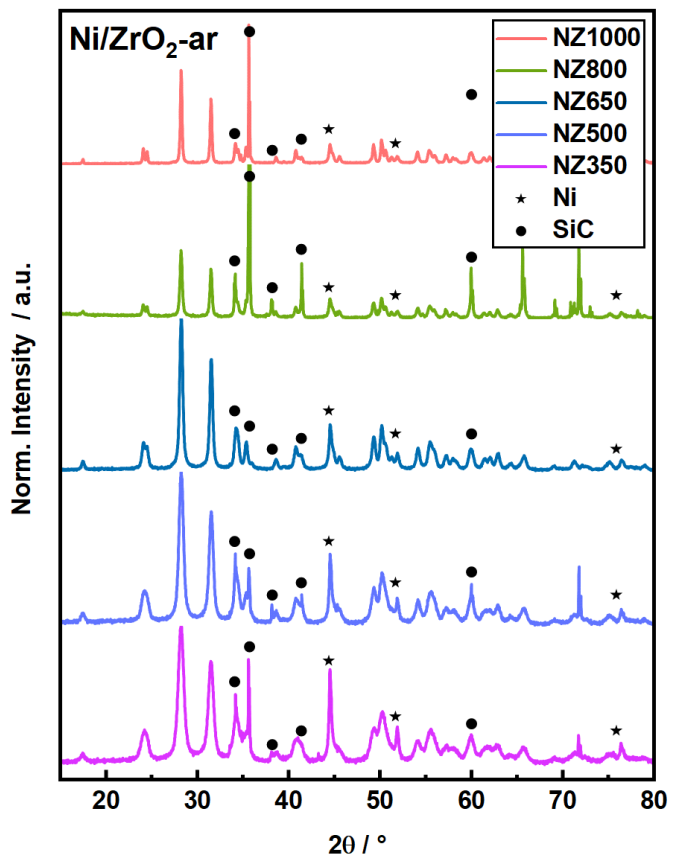


Figure S 9 XRD patterns of the spent Ni/ZrO₂ catalysts after catalytic tests in CO₂ methanation. The present Ni is marked with black stars and present SiC is marked with black circles. SiC is used as inert material in the reactor and could not be separated completely after reaction.

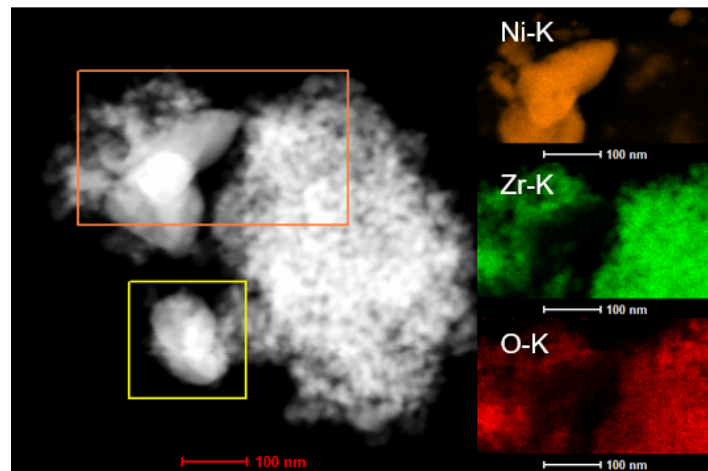


Figure S 10 STEM images with EDX mapping of NZ500 after CO₂ methanation. The orange box indicates the investigated area with EDX, the yellow one is for drift correction.

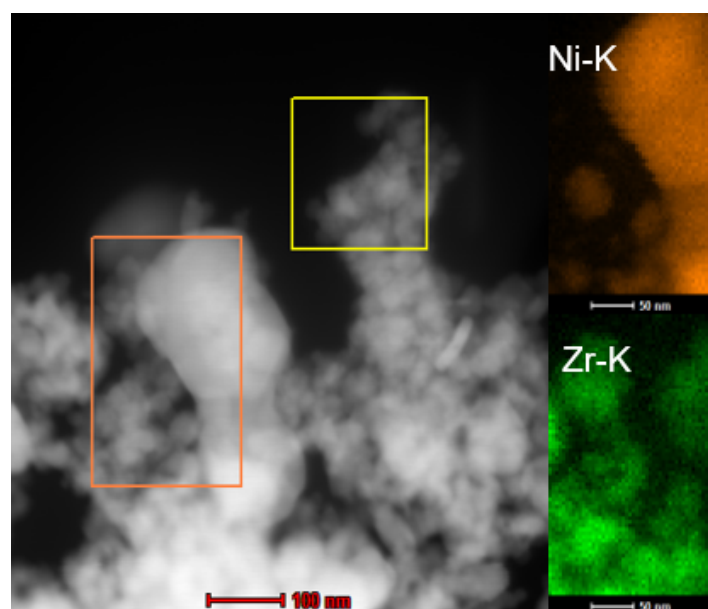


Figure S 11 STEM images with EDX mapping of NZ650 after CO₂ methanation. The orange box indicates the investigated area with EDX, the yellow one is for drift correction.

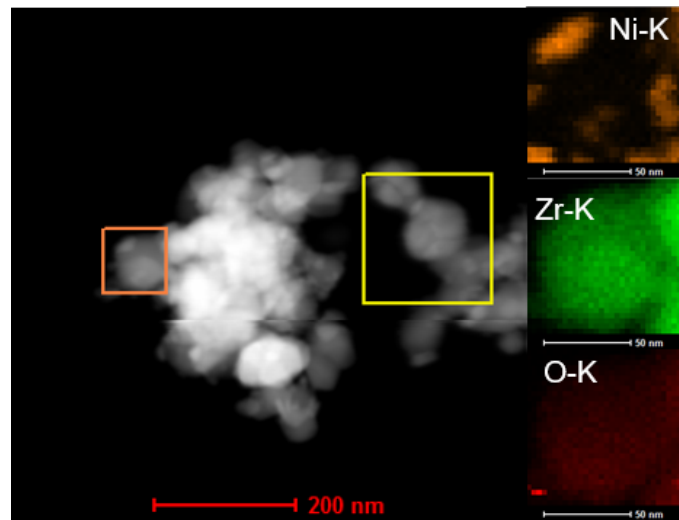


Figure S 12 STEM images with EDX mapping of NZ1000 after CO_2 methanation. The orange box indicates the investigated area with EDX, the yellow one is for drift correction.

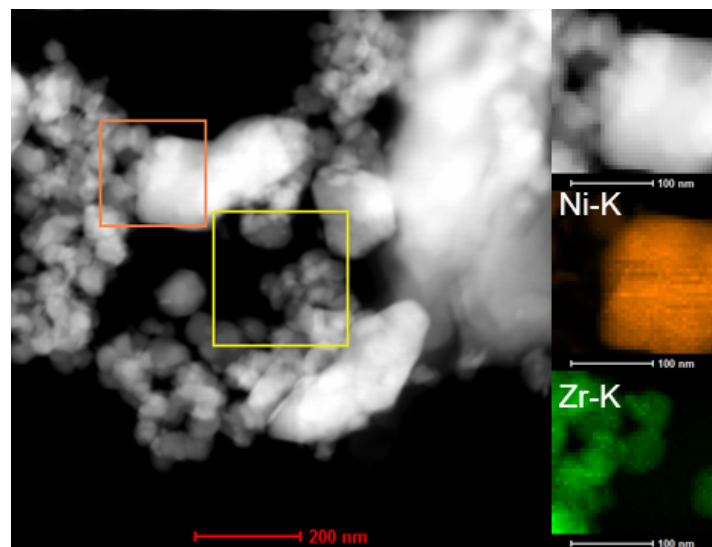


Figure S 13 STEM images with EDX mapping of NZ1000 after CO_2 methanation. The orange box indicates the investigated area with EDX, the yellow one is for drift correction.

2 Laboratory catalytic testing

For the testing of the catalytic performance a continuous flow setup was used.

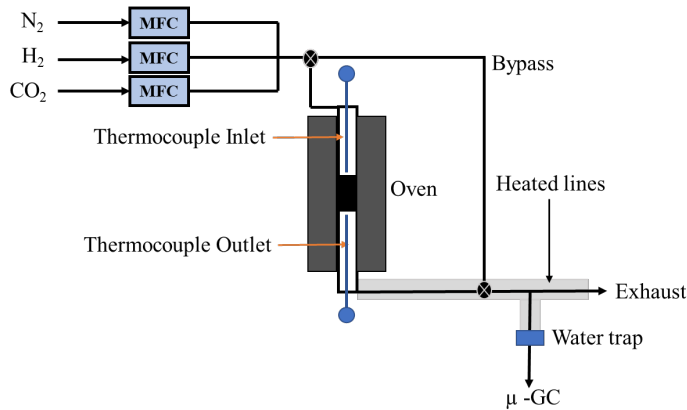


Figure S 14 Scheme of the continuous flow laboratory setup used for testing the catalysts in CO₂ methanation.

The conversion of CO₂ was calculated analogous to earlier measurements by Mutz *et al.*¹ using N₂ as internal standard (eq.1).

$$X_{CO_2} = 1 - \frac{CO_2^{out} \cdot N_2^{in}}{CO_2^{in} \cdot N_2^{out}} \quad (1)$$

The selectivity of CH₄ and CO was calculated according to equations 2 and 3.

$$S_{CH_4} = \frac{CH_4}{CH_4 + CO} \quad (2)$$

$$S_{CO} = \frac{CO}{CH_4 + CO} \quad (3)$$

The yield of CH₄ and CO was determined by multiplication of the conversion of CO₂ and the selectivity of CH₄ and CO (4,5).

$$Y_{CH_4} = X_{CO_2} \cdot S_{CH_4} \quad (4)$$

$$Y_{CO} = X_{CO_2} \cdot S_{CO} \quad (5)$$

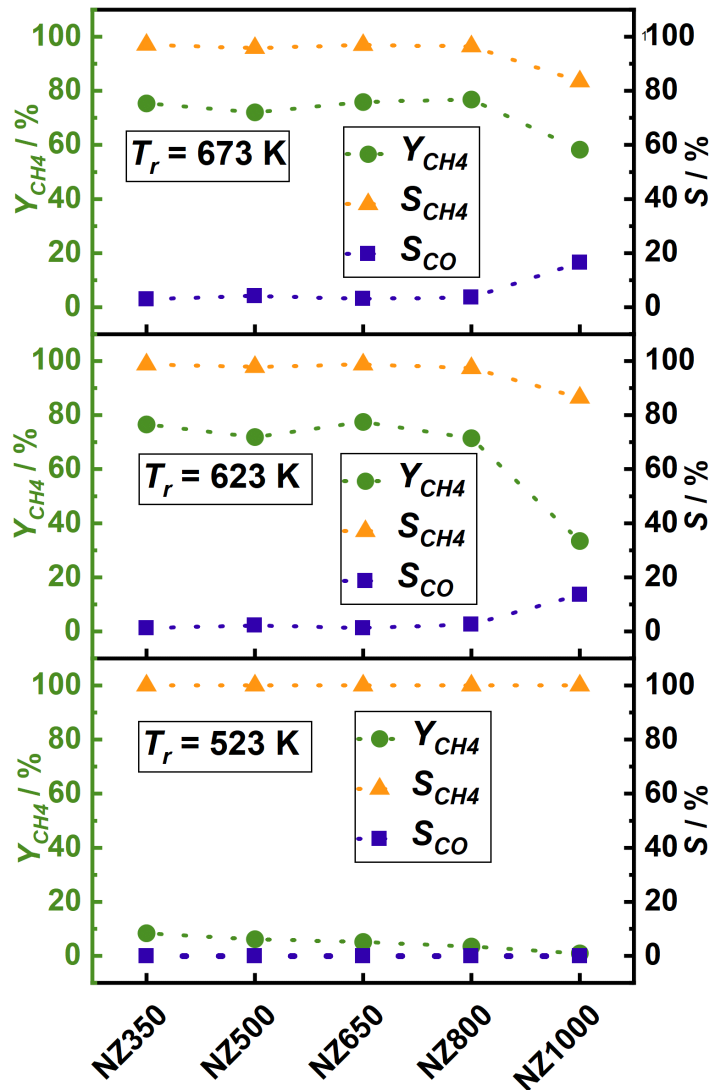


Figure S 15 Catalytic performance of the Ni/ZrO₂ catalyst series during CO₂ methanation at 523 K, 623 K and 673 K. Calculated CH₄ yield (green, left side) and selectivity towards CH₄ (orange) and CO (blue).

The equation used for the calculation of TOF is depicted in equation (eq 6). Hereby, $V_{CO_2}^{in}$ is the flow rate of CO_2 (60 mL min^{-1}), Y_{CH_4} is the CH_4 yield and V_m is the ideal molar gas volume.

$$TOF = \frac{V_{CO_2}^{in} \cdot Y_{CH_4}}{V_m \cdot n_{active}} \quad (6)$$

The last parameter is n_{active} which was calculated according to equation (eq 7) containing the variables of mass (m), molar mass (M), metal loading (L) and dispersion (D) of Ni. All except for the dispersion are known.

$$n_{active} = \frac{m \cdot L \cdot D}{M} \quad (7)$$

The dispersion D was calculated out of its relation with the Sauter diameter (d_{VA}) and atomic diameter d_{At} (eq 9)². For Ni the atomic diameter of 124.6 pm was used³. The Sauter diameter can be calculated out of the volume (V) and the surface area (A) of a sphere with the crystallite sizes obtained by XRD. Since from TEM no statistic relevant particle distribution and sizes could be obtained, and XRD represents the average size it is used for the TOF calculations.

$$d_{VA} = \frac{6V}{A} \quad (8)$$

$$\frac{d_{VA}}{d_{At}} = \frac{3.32}{D} \quad (9)$$

3 Operando SPXRD experiments

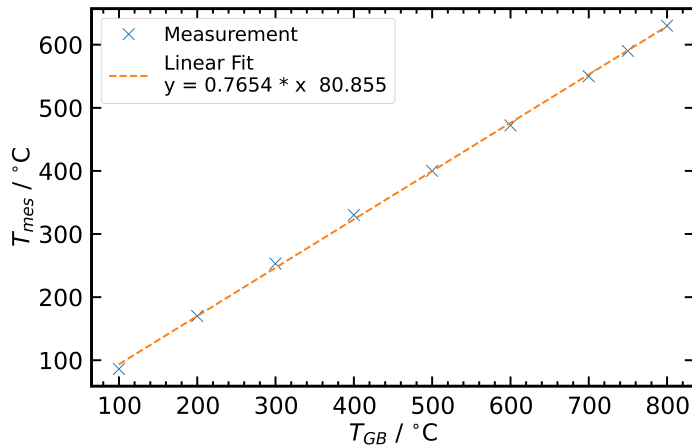


Figure S 16 Calibration of the hot-air blower temperature T_{GB} with the measured temperature inside an empty quartz capillary T_{mes} using a type-K thermocouple.

Online mass spectrometry (MS) was used to quantify the activity of the catalysts during *operando* SPXRD experiments. Selected MS traces normalized by the He ion current are shown in Figure S 17,19,21,23,25 with highlighted regions of activation (blue), reaction (green) and thermal deactivation under reaction conditions (red). The activity in form of conversion X_i of CO_2 and H_2 was determined as described in the main paper, by dividing the normalized ion current of the respective MS traces with the base line value at the end of the experiment. The obtained X_{CO_2} and X_{H_2} during reaction conditions and thermal deactivation cycles for the catalysts are shown in Figure S 18,20,22,24,26. Furthermore, the X_{CO_2} and X_{H_2} conversion for each of the reaction steps R1-4 are summarized in Figure S 27,28, respectively.

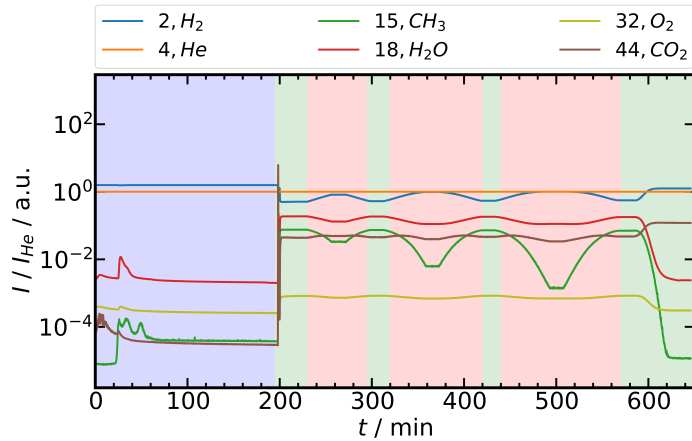


Figure S 17 Selected MS traces and assigned compounds during *operando* SPXRD experiments of NZ350. All traces were normalized by the He trace. Activation conditions of 25 % H_2/He (blue area), reaction conditions of 5 % $\text{CO}_2/20\% \text{H}_2/\text{He}$ (green area) and thermal deactivation cycles under reaction conditions (red area) with a total gas flow of 10 mL min^{-1} .

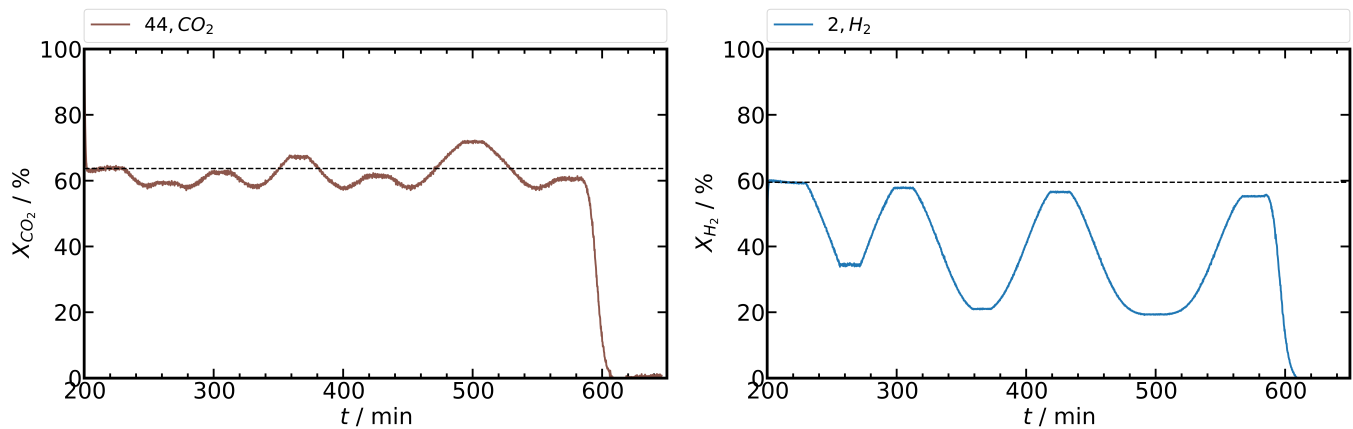


Figure S 18 CO_2 and H_2 conversion from MS data during *operando* SPXRD experiments of NZ350 under reaction conditions of 5% CO_2 /20% H_2 /He and thermal deactivation cycles under reaction conditions.

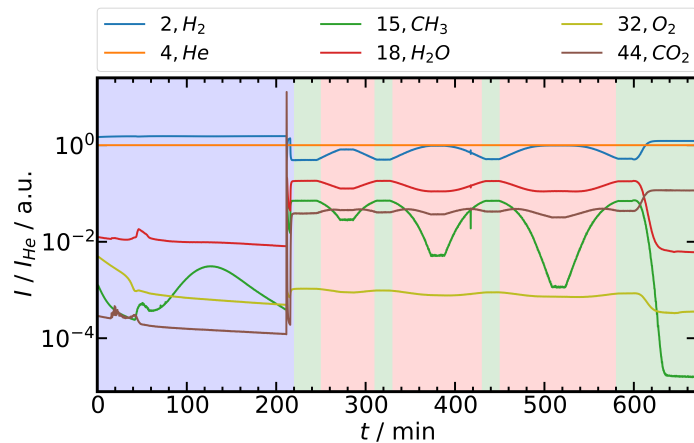


Figure S 19 Selected MS traces and assigned compounds during *operando* SPXRD experiments of NZ500. All traces were normalized by the He trace. Activation conditions of 25% H_2 /He (blue area), reaction conditions of 5% CO_2 /20% H_2 /He (green area) and thermal deactivation cycles under reaction conditions (red area) with a total gas flow of 10 mL min⁻¹.

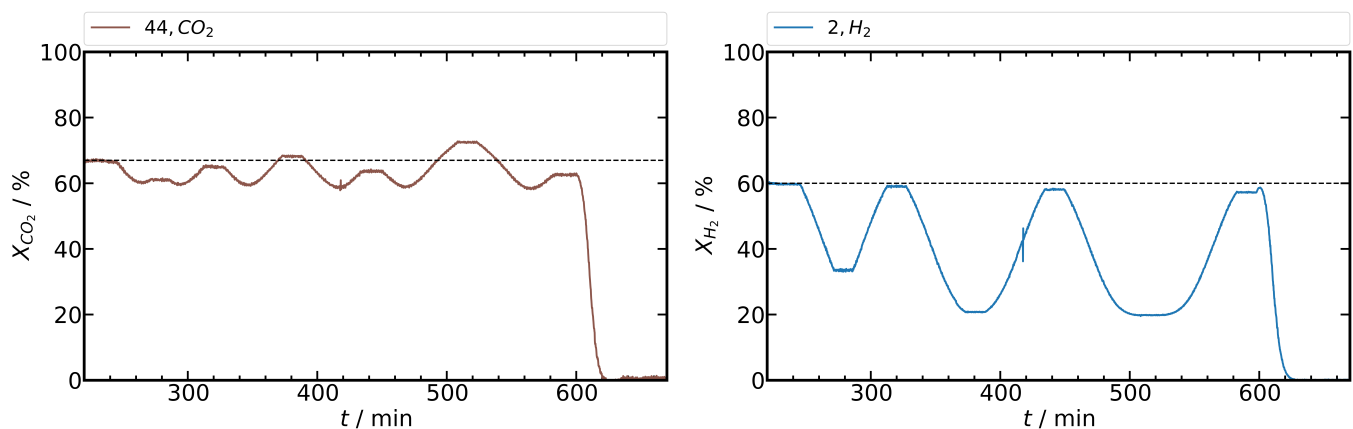


Figure S 20 CO_2 and H_2 conversion from MS data during *operando* SPXRD experiments of NZ500 under reaction conditions of 5% CO_2 /20% H_2 /He and thermal deactivation cycles under reaction conditions.

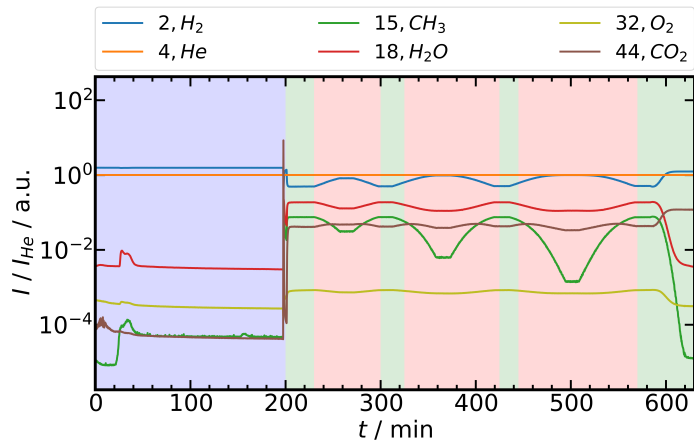


Figure S 21 Selected MS traces and assigned compounds during *operando* SPXRD experiments of NZ650. All traces were normalized by the He trace. Activation conditions of 25%H₂/He (blue area), reaction conditions of 5%CO₂/20%H₂/He (green area) and thermal deactivation cycles under reaction conditions (red area) with a total gas flow of 10 mL min⁻¹.

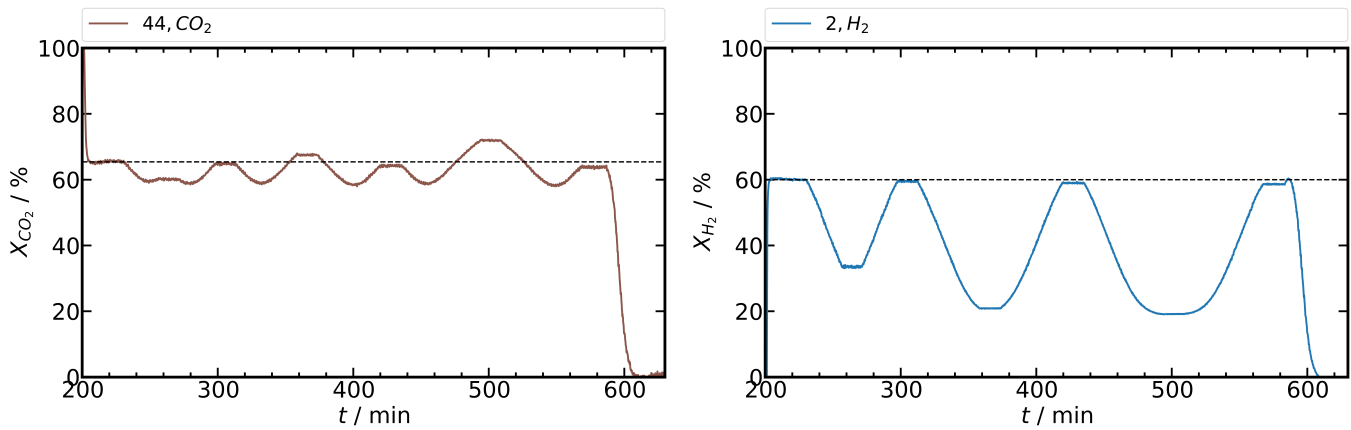


Figure S 22 CO₂ and H₂ conversion from MS data during *operando* SPXRD experiments of NZ650 under reaction conditions of 5%CO₂/20%H₂/He and thermal deactivation cycles under reaction conditions.

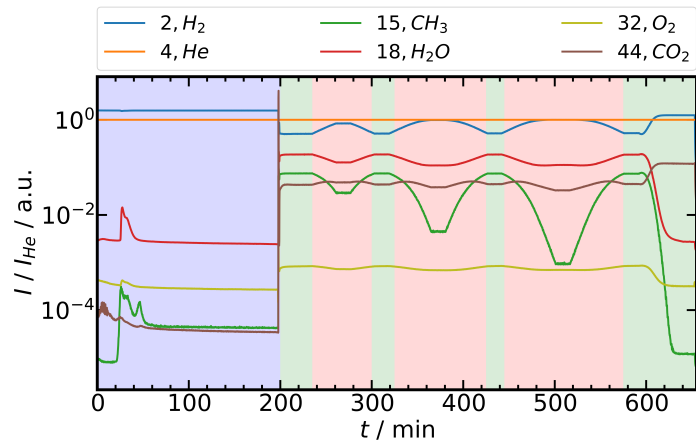


Figure S 23 Selected MS traces and assigned compounds during *operando* SPXRD experiments of NZ800. All traces were normalized by the He trace. Activation conditions of 25%H₂/He (blue area), reaction conditions of 5%CO₂/20%H₂/He (green area) and thermal deactivation cycles under reaction conditions (red area) with a total gas flow of 10 mL min⁻¹.

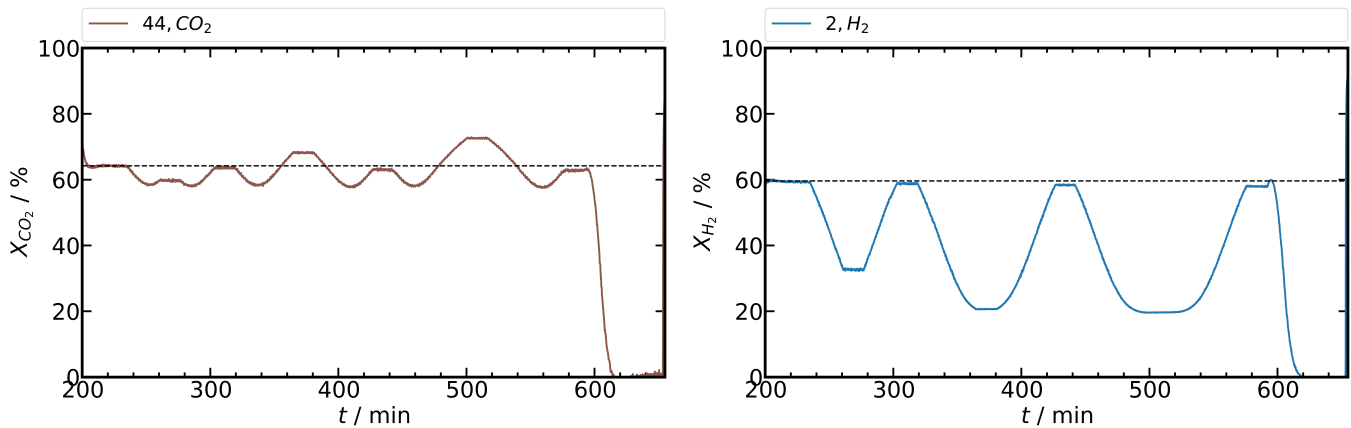


Figure S 24 CO₂ and H₂ conversion from MS data during *operando* SPXRD experiments of NZ800 under reaction conditions of 5%CO₂/20%H₂/He and thermal deactivation cycles under reaction conditions.

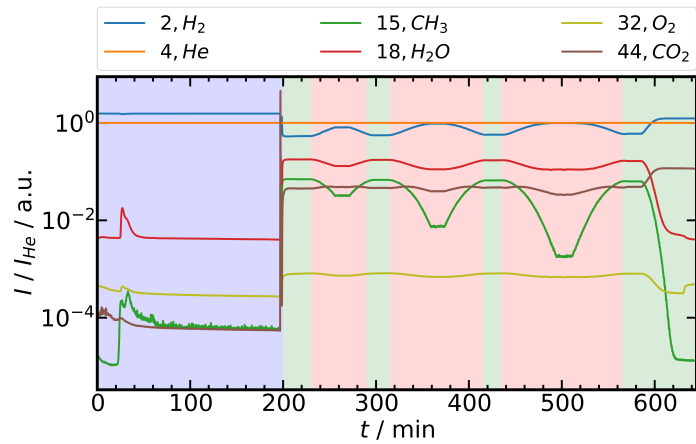


Figure S 25 Selected MS traces and assigned compounds during *operando* SPXRD experiments of NZ1000. All traces were normalized by the He trace. Activation conditions of 25 %H₂/He (blue area), reaction conditions of 5 %CO₂/20 %H₂/He (green area) and thermal deactivation cycles under reaction conditions (red area) with a total gas flow of 10 mL min⁻¹.

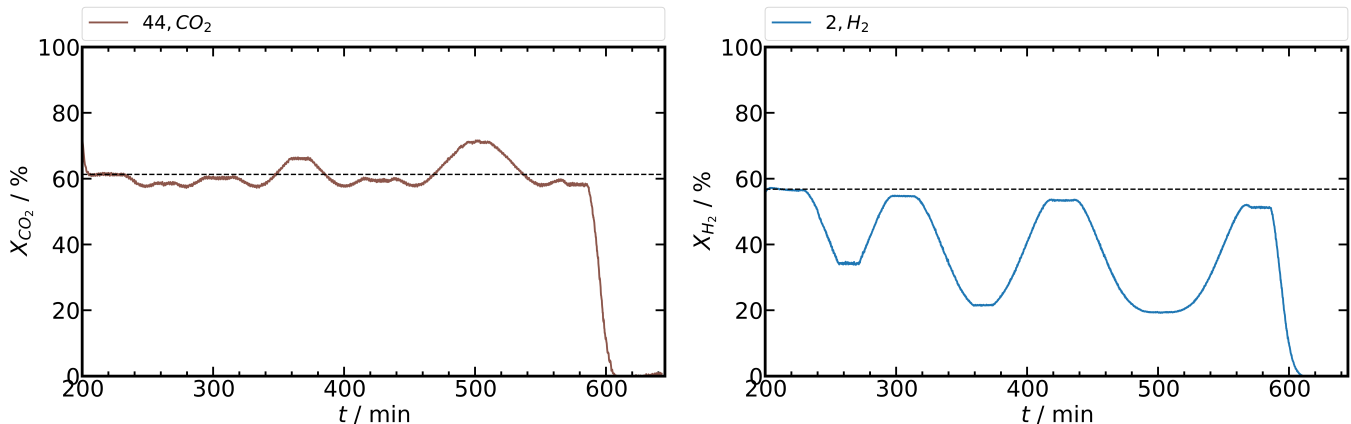


Figure S 26 CO₂ and H₂ conversion from MS data during *operando* SPXRD experiments of NZ1000 under reaction conditions of 5 %CO₂/20 %H₂/He and thermal deactivation cycles under reaction conditions.

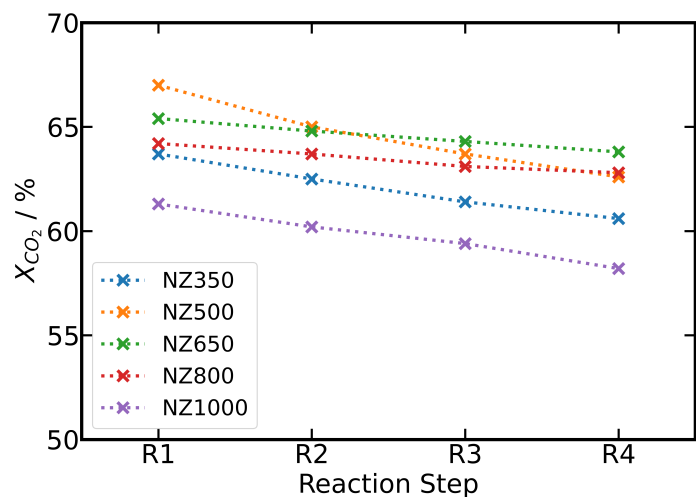


Figure S 27 CO₂ conversion during *operando* SPXRD experiments depending on the reaction step R1 to R4 for the different catalysts.

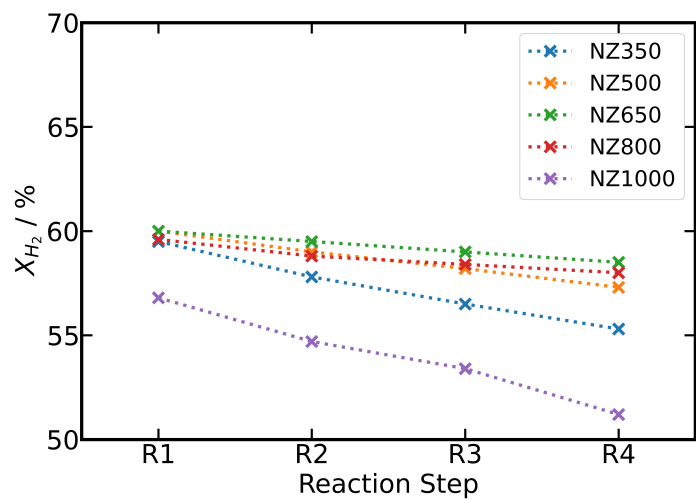


Figure S 28 H_2 conversion during *operando* SPXRD experiments depending on the reaction step R1 to R4 for the different catalysts.

4 Rietveld refinements of the laboratory PXRD and SPXRD experiments

Rietveld refinements^{4,5} of the measured *operando* SPXRD and laboratory PXRD measurements were performed using Topas (v.6, Bruker AXS).⁶ In both cases a measured LaB₆ NIST 640b standard was used to derive an instrumental profile function, described by a pseudo-Voigt Thompson-Cox Hastings peak shape (*operando* SPXRD) or via the fundamental parameters approach for the laboratory diffractometer. A 6th order polynomial was used to describe the background of the diffraction patterns. Refinements of the SPXRD were performed for a Q range of 0.8 to 6.0 Å⁻¹. A micro-structure analysis was performed using the double-Voigt approach by Balzar as implemented in Topas to describe crystallite size (L_{vol}) and strain (η).⁷ The SPXRD profile of the catalysts were refined by employing each a Lorentzian and Gaussian component for size and strain in case of the monoclinic ZrO₂ phase, while for the Ni and NiO phases the size was described with a Lorentzian and the strain with a Gaussian component. This was required due to the small number of reflections of the Ni and NiO phases in the investigate Q space and is a common strategy to prevent parameters running into non-physical values during refinement.^{8,9} The laboratory PXRD are used to compare catalysts before and after testing. The discussion of crystallite size changes and sintering is only based on the SPXRD data

The monoclinic ZrO₂ phase was described by the structure reported by Smith *et al.*¹⁰, tetragonal ZrO₂ phase based on a structure by Bondars *et al.*¹¹, NiO phase could be described with a structure by Rodic *et al.*¹² and the Ni phase with a structure by Rouquette *et al.*¹³ For laboratory PXRD, lattice parameters, micro-structural parameters and atom coordinates were refined, while thermal displacement parameters could not be refined. Results of the refinements of the laboratory PXRD are summarized in Table S 23,4,5,6,7.

For SPXRD refinements lattice parameters, micro-structural parameters and atom coordinates were refined, while thermal displacement parameters were allowed to be refined restrained an a range of 0 to 5 Å², with only one B_{iso} parameter used for both O positions. *Ex situ* SPXRD of the pure supports are shown in Figure S 29,30,31,32,33 and the refinements results are summarized in Table S 8. For the *operando* SPXRD sequential Rietveld refinements were performed by adapting templates available from the Topas wiki website.¹⁴ Selected refined diffraction patterns of the initial state and the final state after *operando* SPXRD for the catalysts are shown in Figure S 34,35,36,37,38 with the respective refinement results summarized in Table S 9,10,11,12,13. The evolution of the GOF during sequential refinements is shown in Figure S 40, it should be noted that the abrupt changes can be related to different measurement conditions between activation, reaction conditions and final cool-down. For activation and cool-down the acquisition time was 9 s and for reaction conditions and thermal deactivation cycles 3 s. The sequentially refined lattice parameters for the ZrO₂ phase of the catalysts are shown in Figure S 41,42,43,44, the B_{iso} in Figure S 45,46. For the Ni phase the sequentially refined lattice parameter is shown in Figure S 47 and the B_{iso} in Figure S 48

Table S 2 Rietveld refinement results for the laboratory PXRD of the pure support materials Z350-1000.

support	Z350	Z500	Z650	Z800	Z1000
phase	m-ZrO ₂	t-ZrO ₂	m-ZrO ₂	m-ZrO ₂	m-ZrO ₂
space group	<i>P</i> 2 ₁ / <i>c</i>	<i>P</i> 4 ₂ / <i>nmc</i>	<i>P</i> 2 ₁ / <i>c</i>	<i>P</i> 2 ₁ / <i>c</i>	<i>P</i> 2 ₁ / <i>c</i>
<i>R</i> _{exp} / %	1.92		1.92	1.90	1.92
<i>R</i> _{wp} / %	2.37		2.79	2.78	3.29
<i>R</i> _p / %	1.89		2.16	2.17	2.56
<i>GOF</i> / %	1.23		1.45	1.46	1.68
<i>ω</i> / wt.%	96.49(10)	3.51(10)	100	100	100
<i>L</i> _{vol} / nm	9.45(8)	8.9(4)	13.23(11)	22.9(2)	40.9(5)
<i>η</i> /	0.00042(4)	-	0.00015(2)	0.000116(15)	0.000132(10)
<i>a</i> / Å	5.1550(4)	3.6110(17)	5.14991(13)	5.15190(15)	5.14954(10)
<i>b</i> / Å	5.2123(4)	-	5.20976(14)	5.21400(17)	5.21113(11)
<i>c</i> / Å	5.3211(4)	5.169(5)	5.31802(15)	5.32075(18)	5.31963(11)
<i>β</i> / °	99.244(4)	-	99.2351(13)	99.2182(15)	99.1995(10)
atom parameters m-ZrO ₂					
Zr1					
<i>x</i>	0.27711(16)		0.27618(15)	0.27595(13)	0.27592(11)
<i>y</i>	0.03992(14)		0.03967(13)	0.03990(11)	0.03990(9)
<i>z</i>	0.20932(17)		0.20962(15)	0.20995(12)	0.20964(10)
<i>B</i> _{iso} / Å ²	0		0	0	0
<i>occ</i>	1		1	1	1
O1					
<i>x</i>	0.0722(9)		0.0734(9)	0.0747(7)	0.0746(6)
<i>y</i>	0.3274(8)		0.3282(7)	0.3310(6)	0.3323(5)
<i>z</i>	0.3467(7)		0.3445(7)	0.3445(6)	0.3445(6)
<i>B</i> _{iso} / Å ²	0		0	0	0
<i>occ</i>	1		1	1	1
O2					
<i>x</i>	0.4508(10)		0.4529(9)	0.4524(7)	0.4511(6)
<i>y</i>	0.7554(6)		0.7555(5)	0.7554(5)	0.7553(4)
<i>z</i>	0.4771(12)		0.4779(12)	0.4809(10) 0.4806(9)	0.4804(10)
<i>B</i> _{iso} / Å ²	0		0	0	0
<i>occ</i>	1		1	1	1
atom parameters t-ZrO ₂					
Zr1					
<i>x</i>	3/4		n.a.	n.a.	n.a.
<i>y</i>	1/4		n.a.	n.a.	n.a.
<i>z</i>	1/4		n.a.	n.a.	n.a.
<i>B</i> _{iso} / Å ²	0.48		n.a.	n.a.	n.a.
<i>occ</i>	1		n.a.	n.a.	n.a.
O1					
<i>x</i>	1/4		n.a.	n.a.	n.a.
<i>y</i>	1/4		n.a.	n.a.	n.a.
<i>z</i>	0.45450		n.a.	n.a.	n.a.
<i>B</i> _{iso} / Å ²	0		n.a.	n.a.	n.a.
<i>occ</i>	1		n.a.	n.a.	n.a.

Table S 3 Rietveld refinement results for the laboratory PXRD of the NZ350 catalysts in the initial state and after laboratory CO₂ methanation reaction

	NZ350 initial		NZ350 after	
phase	m-ZrO ₂	NiO	m-ZrO ₂	Ni
space group	<i>P</i> 2 ₁ / <i>c</i>	<i>R</i> ̄3 <i>m</i>	<i>P</i> 2 ₁ / <i>c</i>	<i>F</i> m̄3 <i>m</i>
<i>R</i> _{exp} / %	1.51		1.74	
<i>R</i> _{wp} / %	1.86		2.31	
<i>R</i> _p / %	1.45		1.72	
<i>GOF</i> / %	1.24		1.35	
<i>ω</i> / wt.%	82.48(12)	17.52(12)	88.11(10)	11.89(10)
<i>L</i> _{vol} / nm	10.36(11)	10.73(15)	10.08(12)	33.5(7)
<i>η</i> /	0.00044(4)	-	0.00004(5)	-
<i>a</i> / Å	5.1537(4)	2.9622(4)	5.1540(5)	3.5266(2)
<i>b</i> / Å	5.2123(5)	-	5.2118(6)	-
<i>c</i> / Å	5.3201(5)	7.221(2)	5.3205(6)	-
<i>β</i> / °	99.190(4)	-	99.198(5)	-
	Zr1	Ni1	Zr1	Ni 1
<i>x</i>	0.2765(2)	0	0.2759(3)	0
<i>y</i>	0.03882(17)	0	0.0387(2)	0
<i>z</i>	0.2090(2)	0	0.2095(3)	0
<i>B</i> _{iso} / Å ²	0	0	0	0.0058
<i>occ</i>	1	1	1	1
	O1	O1	O1	
<i>x</i>	0.0746(11)	0	0.0775(16)	
<i>y</i>	0.3250(9)	0	0.3324(12)	
<i>z</i>	0.3465(9)	1/2	0.3356(13)	
<i>B</i> _{iso} / Å ²	0	0	0	
<i>occ</i>	1	1	1	
	O2		O2	
<i>x</i>	0.4535(12)		0.4534(16)	
<i>y</i>	0.7545(7)		0.7554(9)	
<i>z</i>	0.4745(15)		0.466(2)	
<i>B</i> _{iso} / Å ²	0		0	
<i>occ</i>	1		1	

Table S 4 Rietveld refinement results for the laboratory PXRD of the NZ500 catalysts in the initial state and after laboratory CO₂ methanation reaction

	NZ500 initial		NZ500 after	
phase	m-ZrO ₂	NiO	m-ZrO ₂	Ni
space group	<i>P</i> 2 ₁ / <i>c</i>	<i>R</i> ̄3 <i>m</i>	<i>P</i> 2 ₁ / <i>c</i>	<i>F</i> m̄3 <i>m</i>
<i>R</i> _{exp} / %	1.53		1.71	
<i>R</i> _{wp} / %	1.96		2.69	
<i>R</i> _p / %	1.52		1.89	
<i>GOF</i> / %	1.28		1.57	
<i>ω</i> / wt.%	83.35(13)	16.65(13)	89.69(11)	10.31(11)
<i>L</i> _{vol} / nm	13.64(14)	9.61(15)	13.32(17)	32.3(8)
<i>η</i> /	0.00028(3)	-	0.00001(4)	-
<i>a</i> / Å	5.1515(3)	2.9623(5)	5.1520(4)	3.52709(19)
<i>b</i> / Å	5.2131(3)	-	5.2119(5)	-
<i>c</i> / Å	5.3196(3)	7.222(3)	5.3214(5)	-
<i>β</i> / °	99.209(3)	-	99.219(4)	-
	Zr1	Ni1	Zr1	Ni 1
<i>x</i>	0.27633(18)	0	0.2770(3)	0
<i>y</i>	0.03958(15)	0	0.0398(2)	0
<i>z</i>	0.21005(17)	0	0.2104(2)	0
<i>B</i> _{iso} / Å ²	0	0	0	0.0058
<i>occ</i>	1	1	1	1
	O1	O1	O1	
<i>x</i>	0.0755(10)	0	0.0682(19)	
<i>y</i>	0.3287(8)	0	0.3365(12)	
<i>z</i>	0.3453(8)	1/2	0.3351(13)	
<i>B</i> _{iso} / Å ²	0	0	0	
<i>occ</i>	1	1	1	
	O2		O2	
<i>x</i>	0.4529(10)		0.463(2)	
<i>y</i>	0.7548(6)		0.7542(9)	
<i>z</i>	0.4769(14)		0.462(2)	
<i>B</i> _{iso} / Å ²	0		0	
<i>occ</i>	1		1	

Table S 5 Rietveld refinement results for the laboratory PXRD of the NZ650 catalysts in the initial state and after laboratory CO₂ methanation reaction

	NZ650 initial		NZ650 after	
phase	m-ZrO ₂	NiO	m-ZrO ₂	Ni
space group	<i>P</i> 2 ₁ / <i>c</i>	<i>R</i> ̄3 <i>m</i>	<i>P</i> 2 ₁ / <i>c</i>	<i>F</i> m̄3 <i>m</i>
<i>R</i> _{exp} / %	1.51		1.54	
<i>R</i> _{wp} / %	1.93		2.02	
<i>R</i> _p / %	1.50		1.56	
<i>GOF</i> / %	1.28		1.31	
<i>ω</i> / wt.%	81.12(13)	18.88(13)	88.17(9)	11.83(9)
<i>L</i> _{vol} / nm	23.0(2)	10.33(14)	22.1(2)	24.6(4)
<i>η</i> /	0.000146(18)	-	0.000046(18)	-
<i>a</i> / Å	5.15214(18)	2.9628(5)	5.15125(18)	3.52715(12)
<i>b</i> / Å	5.2148(2)	-	5.2140(2)	-
<i>c</i> / Å	5.3208(2)	7.230(3)	5.3193(2)	-
<i>β</i> / °	99.2074(17)	-	99.2084(18)	-
	Zr1	Ni1	Zr1	Ni 1
<i>x</i>	0.27616(15)	0	0.27610(16)	0
<i>y</i>	0.03987(12)	0	0.03967(13)	0
<i>z</i>	0.21012(14)	0	0.21001(14)	0
<i>B</i> _{iso} / Å ²	0	0	0	0.0058
<i>occ</i>	1	1	1	1
	O1	O1	O1	
<i>x</i>	0.0748(8)	0	0.0745(8)	
<i>y</i>	0.3314(7)	0	0.3316(7)	
<i>z</i>	0.3442(7)	1/2	0.3426(7)	
<i>B</i> _{iso} / Å ²	0	0	0	
<i>occ</i>	1	1	1	
	O2		O2	
<i>x</i>	0.4507(8)		0.4524(9)	
<i>y</i>	0.7548(5)		0.7547(5)	
<i>z</i>	0.4800(12)		0.4815(14)	
<i>B</i> _{iso} / Å ²	0		0	
<i>occ</i>	1		1	

Table S 6 Rietveld refinement results for the laboratory PXRD of the NZ800 catalysts in the initial state and after laboratory CO₂ methanation reaction

	NZ800 initial		NZ800 after	
phase	m-ZrO ₂	NiO	m-ZrO ₂	Ni
space group	<i>P</i> 2 ₁ / <i>c</i>	<i>R</i> ̄3 <i>m</i>	<i>P</i> 2 ₁ / <i>c</i>	<i>F</i> m̄3 <i>m</i>
<i>R</i> _{exp} / %	1.49		2.33	
<i>R</i> _{wp} / %	1.83		4.55	
<i>R</i> _p / %	1.43		3.11	
<i>GOF</i> / %	1.23		1.96	
<i>ω</i> / wt.%	79.78(14)	20.22(14)	88.0(3)	12.0(3)
<i>L</i> _{vol} / nm	44.5(6)	8.10(11)	34.1(13)	31.2(17)
<i>η</i> /	0.000204(12)	-	0.00000(5)	-
<i>a</i> / Å	5.15138(12)	2.9652(5)	5.1504(4)	3.5280(3)
<i>b</i> / Å	5.21357(13)	-	5.2121(5)	-
<i>c</i> / Å	5.32117(13)	7.221(3)	5.3259(5)	-
<i>β</i> / °	99.1923(11)	-	99.193(4)	-
	Zr1	Ni1	Zr1	Ni 1
<i>x</i>	0.27558(13)	0	0.2758(6)	0
<i>y</i>	0.03936(11)	0	0.0383(4)	0
<i>z</i>	0.20960(12)	0	0.2133(5)	0
<i>B</i> _{iso} / Å ²	0	0	0	0.0058
<i>occ</i>	1	1	1	1
	O1	O1	O1	
<i>x</i>	0.0749(7)	0	0.091(4)	
<i>y</i>	0.3334(6)	0	0.364(2)	
<i>z</i>	0.3437(6)	1/2	0.311(3)	
<i>B</i> _{iso} / Å ²	0	0	0	
<i>occ</i>	1	1	1	
	O2		O2	
<i>x</i>	0.4535(7)		0.458(3)	
<i>y</i>	0.7555(4)		0.7525(19)	
<i>z</i>	0.4788(10)		0.395(3)	
<i>B</i> _{iso} / Å ²	0		0	
<i>occ</i>	1		1	

Table S 7 Rietveld refinement results for the laboratory PXRD of the NZ1000 catalysts in the initial state and after laboratory CO₂ methanation reaction

	NZ1000 initial		NZ1000 after	
phase	m-ZrO ₂	NiO	m-ZrO ₂	Ni
space group	<i>P</i> 2 ₁ / <i>c</i>	<i>R</i> ̄3 <i>m</i>	<i>P</i> 2 ₁ / <i>c</i>	<i>F</i> m̄3 <i>m</i>
<i>R</i> _{exp} / %	1.52		1.71	
<i>R</i> _{wp} / %	2.05		2.66	
<i>R</i> _p / %	1.56		3.05	
<i>GOF</i> / %	1.35		1.56	
<i>ω</i> / wt.%	79.97(16)	20.03(16)	87.19(12)	12.81(12)
<i>L</i> _{vol} / nm	95(2)	7.85(12)	76.4(19)	29.4(7)
<i>η</i> /	0.000322(10)	-	0.000173(13)	-
<i>a</i> / Å	5.15062(10)	2.9544(9)	5.15187(12)	3.52826(11)
<i>b</i> / Å	5.21006(11)	-	5.21112(13)	-
<i>c</i> / Å	5.32250(11)	7.265(5)	5.32425(14)	-
<i>β</i> / °	99.1693(10)	-	99.1672(12)	-
	Zr1	Ni1	Zr1	Ni 1
<i>x</i>	0.27614(14)	0	0.27580(18)	0
<i>y</i>	0.03951(11)	0	0.03902(16)	0
<i>z</i>	0.20946(12)	0	0.20949(16)	0
<i>B</i> _{iso} / Å ²	0	0	0	0.0058
<i>occ</i>	1	1	1	1
	O1	O1	O1	
<i>x</i>	0.0750(7)	0	0.0800(9)	
<i>y</i>	0.3326(6)	0	0.3333(8)	
<i>z</i>	0.3439(6)	1/2	0.3380(9)	
<i>B</i> _{iso} / Å ²	0	0	0	
<i>occ</i>	1	1	1	
	O2		O2	
<i>x</i>	0.4500(7)		0.4460(10)	
<i>y</i>	0.7551(5)		0.7555(6)	
<i>z</i>	0.4820(11)		0.4800(16)	
<i>B</i> _{iso} / Å ²	0		0	
<i>occ</i>	1		1	

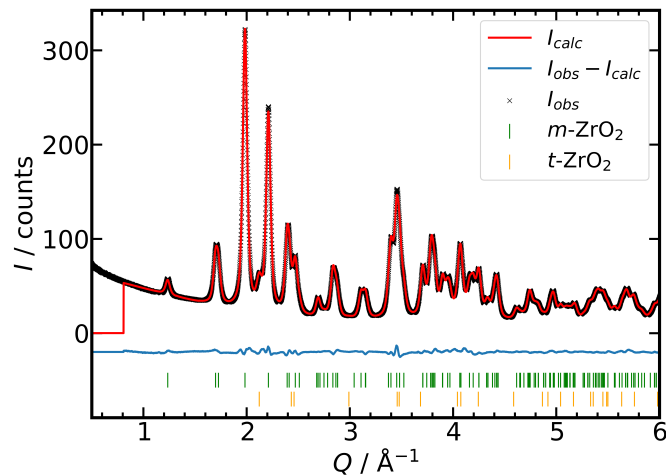


Figure S 29 Rietveld refinement of the measured *ex situ* SPXRD measurement of Z350.

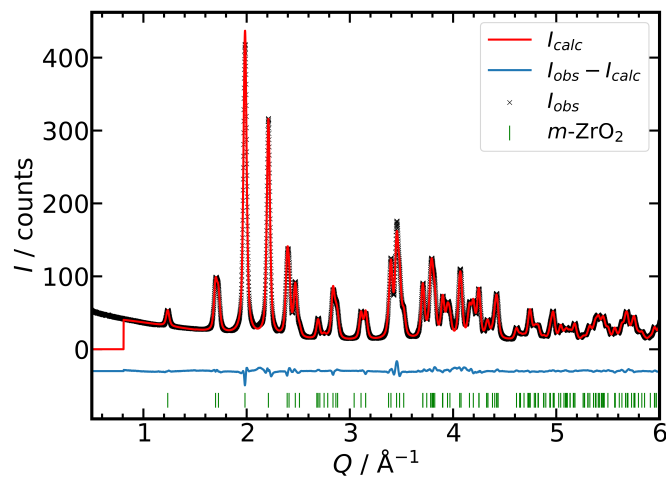


Figure S 30 Rietveld refinement of the measured *ex situ* SPXRD measurement of Z500.

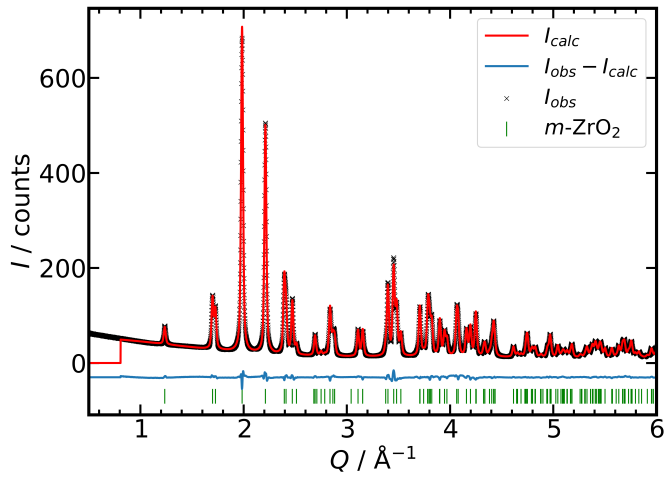


Figure S 31 Rietveld refinement of the measured *ex situ* SPXRD measurement of Z650.

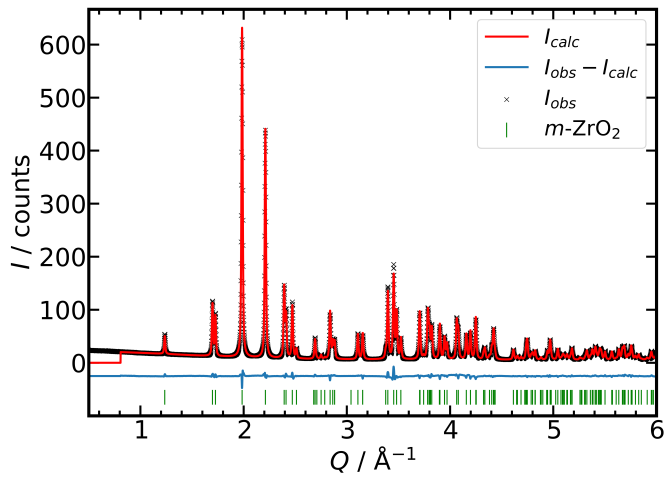


Figure S 32 Rietveld refinement of the measured *ex situ* SPXRD measurement of Z800.

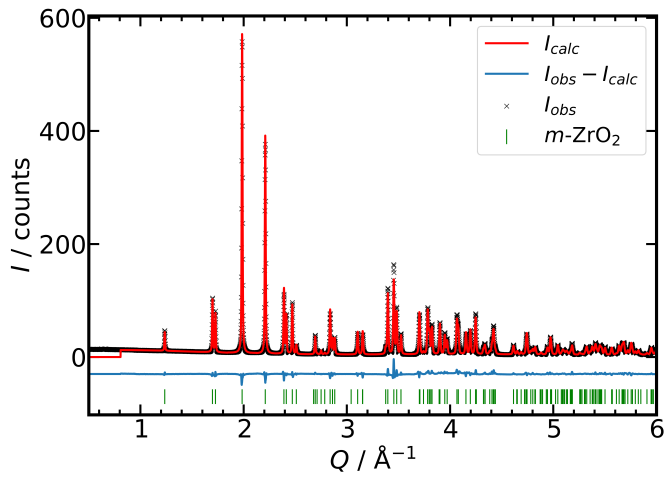


Figure S 33 Rietveld refinement of the measured *ex situ* SPXRD measurement of Z1000.

Table S 8 Rietveld refinement results for the *ex situ* SPXRD of the pure support materials Z350-1000.

support	Z350	Z500	Z650	Z800	Z1000
phase	m-ZrO ₂	t-ZrO ₂	m-ZrO ₂	m-ZrO ₂	m-ZrO ₂
space group	<i>P</i> 2 ₁ / <i>c</i>	<i>P</i> 4 ₂ / <i>nmc</i>	<i>P</i> 2 ₁ / <i>c</i>	<i>P</i> 2 ₁ / <i>c</i>	<i>P</i> 2 ₁ / <i>c</i>
<i>R</i> _{exp} / %	11.50		12.52	12.32	17.76
<i>R</i> _{wp} / %	2.36		3.39	3.23	4.31
<i>R</i> _p / %	1.83		2.46	2.46	5.09
<i>GOF</i> / %	0.21		0.27	0.26	0.24
<i>ω</i> / wt.%	95.47(14)	4.53(14)	100	100	100
<i>L</i> _{vol} / nm	9.63(14)	12.7(12)	13.13(14)	22.8(2)	41.1(6)
<i>η</i> /	0.00098(8)	0.0045(2)	0.00069(4)	0.0002(6)	0.00030(2)
<i>a</i> / Å	5.1508(2)	3.612(2)	5.14991(13)	5.14873(7)	5.14849(6)
<i>b</i> / Å	5.2077(2)	-	5.20976(14)	5.21034(8)	5.20977(6)
<i>c</i> / Å	5.3199(3)	5.165(7)	5.31802(15)	5.31735(8)	5.31872(7)
<i>β</i> / °	99.254(2)	-	99.2351(13)	99.2197(8)	99.1975(6)
atom parameters m-ZrO ₂					
Zr1					
<i>x</i>	0.27526(9)		0.27512(7)	0.27524(7)	0.27515(8)
<i>y</i>	0.03949(8)		0.03917(6)	0.03971(5)	0.03977(6)
<i>z</i>	0.20940(11)		0.20928(8)	0.20913(7)	0.20900(8)
<i>B</i> _{iso} / Å ²	0.00(3)		0.000(17)	0.722(14)	0.651(16)
<i>occ</i>	1		1	1	1
O1					
<i>x</i>	0.0748(7)		0.0762(5)	0.0742(4)	0.0750(5)
<i>y</i>	0.3229(5)		0.3247(4)	0.3284(4)	0.3297(5)
<i>z</i>	0.3472(5)		0.3436(4)	0.3440(4)	0.3451(5)
<i>B</i> _{iso} / Å ²	0.00(9)		0.00(7)	0.90(6)	0.91(7)
<i>occ</i>	1		1	1	1
O2					
<i>x</i>	0.4521(7)		0.4492(5)	0.4495(5)	0.4500(5)
<i>y</i>	0.7583(5)		0.7583(4)	0.7577(3)	0.7574(4)
<i>z</i>	0.4770(7)		0.4788(6)	0.4768(5)	0.4774(6)
<i>B</i> _{iso} / Å ²	0.71(10)		0.42(7)	1.60(6)	1.51(7)
<i>occ</i>	1		1	1	1
atom parameters t-ZrO ₂					
Zr1					
<i>x</i>	3/4		n.a.	n.a.	n.a.
<i>y</i>	1/4		n.a.	n.a.	n.a.
<i>z</i>	1/4		n.a.	n.a.	n.a.
<i>B</i> _{iso} / Å ²	0.00(13)		n.a.	n.a.	n.a.
<i>occ</i>	1		n.a.	n.a.	n.a.
O1					
<i>x</i>	1/4		n.a.	n.a.	n.a.
<i>y</i>	1/4		n.a.	n.a.	n.a.
<i>z</i>	0.417(6)		n.a.	n.a.	n.a.
<i>B</i> _{iso} / Å ²	0.0(8)		n.a.	n.a.	n.a.
<i>occ</i>	1		n.a.	n.a.	n.a.

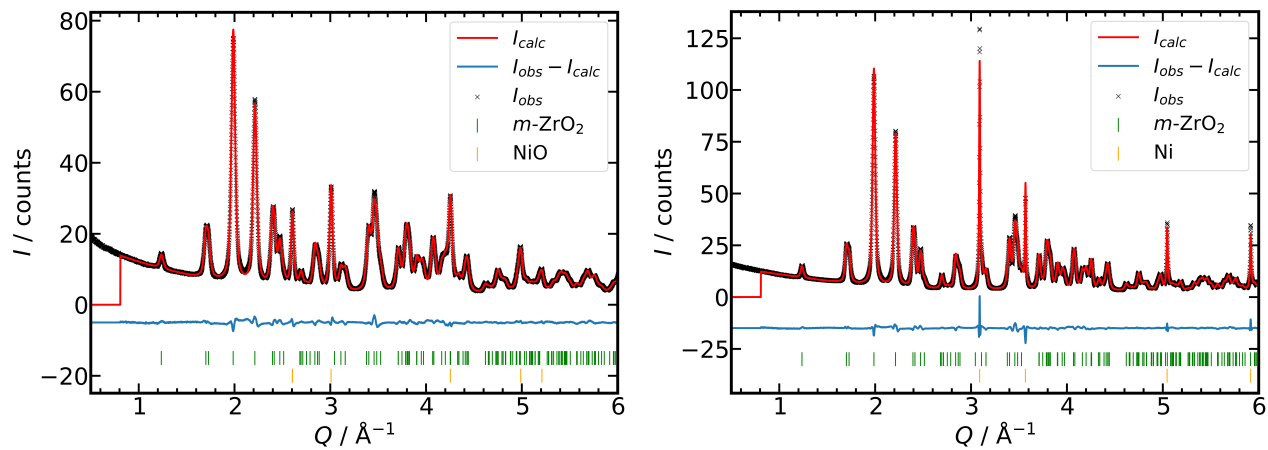


Figure S 34 Rietveld refinements of the initial state before (left) and after (right) *operando* SPXRD experiments of NZ350.

Table S 9 Selected Rietveld refinement results for the NZ350 catalysts in the initial state and after *operando* SPXRD.

	NZ350 initial		NZ350 after	
phase	m-ZrO ₂	NiO	m-ZrO ₂	Ni
space group	<i>P</i> 2 ₁ / <i>c</i>	<i>R</i> ̄3 <i>m</i>	<i>P</i> 2 ₁ / <i>c</i>	<i>F</i> ̄ <i>m</i> 3 <i>m</i>
<i>R</i> _{exp} / %	23.11		24.11	
<i>R</i> _{wp} / %	2.76		3.70	
<i>R</i> _p / %	2.09		2.53	
<i>GOF</i> / %	0.12		0.15	
<i>ω</i> / wt.%	81.36(11)	18.64(11)	86.00(6)	14.00(6)
<i>L</i> _{vol} / nm	10.72(16)	13.94(12)	14.80(17)	37.5(2)
<i>η</i> /	0.00092(9)	0.00128(3)	0.00036(14)	0.00000(3)
<i>a</i> / Å	5.1459(2)	2.954(2)	5.14475(11)	3.52195(4)
<i>b</i> / Å	5.2044(2)	-	5.20276(12)	-
<i>c</i> / Å	5.3126(2)	7.234(11)	5.31441(12)	-
<i>β</i> / °	99.219(2)	-	99.2080(13)	-
	Zr1	Ni1	Zr1	Ni 1
<i>x</i>	0.27536(9)	0	0.27528(8)	0
<i>y</i>	0.03901(8)	0	0.03970(6)	0
<i>z</i>	0.20922(10)	0	0.20951(8)	0
<i>B</i> _{iso} / Å ²	0.45(2)	0.76(3)	0.730(19)	0.692(17)
<i>occ</i>	1	1	1	1
	O1	O1	O1	
<i>x</i>	0.0772(6)	0	0.0731(5)	
<i>y</i>	0.3234(5)	0	0.3268(4)	
<i>z</i>	0.3429(5)	1/2	0.3448(4)	
<i>B</i> _{iso} / Å ²	0.08(8)	0.64(7)	0.45(7)	
<i>occ</i>	1	1	1	
	O2		O2	
<i>x</i>	0.4491(7)		0.4488(6)	
<i>y</i>	0.7580(4)		0.7560(4)	
<i>z</i>	0.4767(7)		0.4731(7)	
<i>B</i> _{iso} / Å ²	0.97(9)		1.03(7)	
<i>occ</i>	1		1	

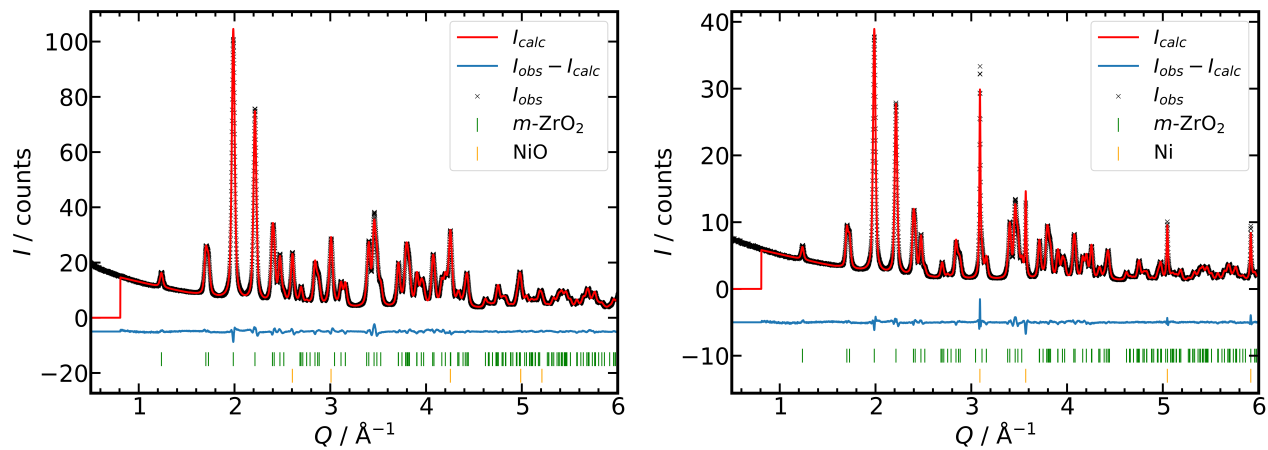


Figure S 35 Rietveld refinements of the initial state before (left) and after (right) *operando* SPXRD experiments of NZ500.

Table S 10 Selected Rietveld refinement results for the NZ500 catalysts in the initial state and after *operando* SPXRD.

	NZ500 initial		NZ500 after	
phase	m-ZrO ₂	NiO	m-ZrO ₂	Ni
space group	<i>P</i> 2 ₁ / <i>c</i>	<i>R</i> ̄3 <i>m</i>	<i>P</i> 2 ₁ / <i>c</i>	<i>F</i> m̄3 <i>m</i>
<i>R</i> _{exp} / %	23.04		39.02	
<i>R</i> _{wp} / %	2.71		3.21	
<i>R</i> _p / %	2.09		2.26	
<i>GOF</i> / %	0.12		0.08	
<i>ω</i> / wt.%	82.84(10)	17.16(10)	87.30(10)	12.70(10)
<i>L</i> _{vol} / nm	14.40(18)	12.93(12)	16.2(3)	33.8(4)
<i>η</i> /	0.000(17)	0.00140(3)	0.00047(10)	0.00000(7)
<i>a</i> / Å	5.14426(13)	2.954(3)	5.14338(17)	3.52124(7)
<i>b</i> / Å	5.20459(15)	-	5.20294(19)	-
<i>c</i> / Å	5.31132(15)	7.236(13)	5.3121(2)	-
<i>β</i> / °	99.2223(14)	-	99.221(2)	-
	Zr1	Ni1	Zr1	Ni 1
<i>x</i>	0.27503(8)	0	0.27512(14)	0
<i>y</i>	0.03932(7)	0	0.03980(11)	0
<i>z</i>	0.20917(8)	0	0.20936(14)	0
<i>B</i> _{iso} / Å ²	0.55(2)	0.85(4)	0.74(3)	0.66(3)
<i>occ</i>	1	1	1	1
	O1	O1	O1	
<i>x</i>	0.0742(5)	0	0.0729(9)	
<i>y</i>	0.3266(4)	0	0.3278(7)	
<i>z</i>	0.3439(4)	1/2	0.3454(7)	
<i>B</i> _{iso} / Å ²	0.42(7)	0.82(7)	0.54(12)	
<i>occ</i>	1	1	1	
	O2		O2	
<i>x</i>	0.4496(6)		0.4499(10)	
<i>y</i>	0.7575(4)		0.7567(7)	
<i>z</i>	0.4789(6)		0.4746(12)	
<i>B</i> _{iso} / Å ²	1.22(7)		1.22(13)	
<i>occ</i>	1		1	

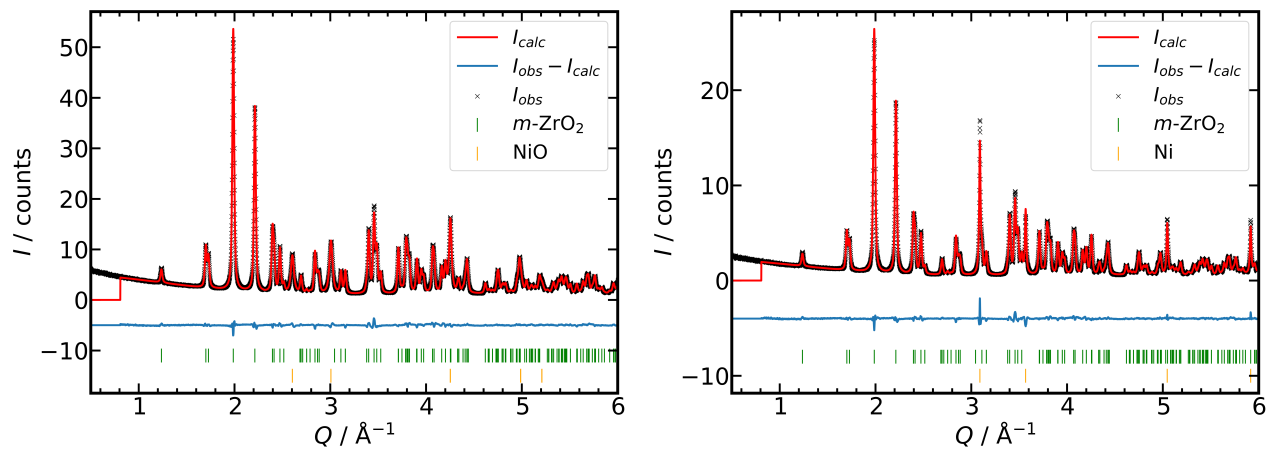


Figure S 36 Rietveld refinements of the initial state before (left) and after (right) *operando* SPXRD experiments of NZ650.

Table S 11 Selected Rietveld refinement results for the NZ650 catalysts in the initial state and after *operando* SPXRD.

	NZ650 initial		NZ650 after	
phase	m-ZrO ₂	NiO	m-ZrO ₂	Ni
space group	<i>P</i> 2 ₁ / <i>c</i>	<i>R</i> ̄3 <i>m</i>	<i>P</i> 2 ₁ / <i>c</i>	<i>F</i> ̄ <i>m</i> 3 <i>m</i>
<i>R</i> _{exp} / %	39.72		58.40	
<i>R</i> _{wp} / %	3.15		3.79	
<i>R</i> _p / %	2.38		2.76	
<i>GOF</i> / %	0.08		0.06	
<i>ω</i> / wt.%	81.13(15)	18.87(15)	85.76(13)	14.24(13)
<i>L</i> _{vol} / nm	21.1(4)	12.87(16)	21.4(5)	27.2(4)
<i>η</i> /	0.00042(4)	0.00121(4)	0.00035(6)	0.00000(13)
<i>a</i> / Å	5.14361(12)	2.955(3)	5.14339(16)	3.52193(8)
<i>b</i> / Å	5.20581(14)	-	5.20514(18)	-
<i>c</i> / Å	5.31131(14)	7.236(13)	5.31185(18)	-
<i>β</i> / °	99.2147(13)	-	99.2190(18)	-
	Zr1	Ni1	Zr1	Ni 1
<i>x</i>	0.27514(11)	0	0.27519(16)	0
<i>y</i>	0.03951(9)	0	0.03964(13)	0
<i>z</i>	0.20902(11)	0	0.20910(15)	0
<i>B</i> _{iso} / Å ²	0.00(2)	0.00(5)	0.00(3)	0.00(4)
<i>occ</i>	1	1	1	1
	O1	O1	O1	
<i>x</i>	0.0736(7)	0	0.0728(10)	
<i>y</i>	0.3292(6)	0	0.3299(9)	
<i>z</i>	0.3445(6)	1/2	0.3459(9)	
<i>B</i> _{iso} / Å ²	0.00(9)	0.19(11)	0.00(13)	
<i>occ</i>	1	1	1	
	O2		O2	
<i>x</i>	0.4498(8)		0.4505(11)	
<i>y</i>	0.7573(6)		0.7565(8)	
<i>z</i>	0.4804(9)		0.4796(14)	
<i>B</i> _{iso} / Å ²	0.86(10)		0.45(14)	
<i>occ</i>	1		1	

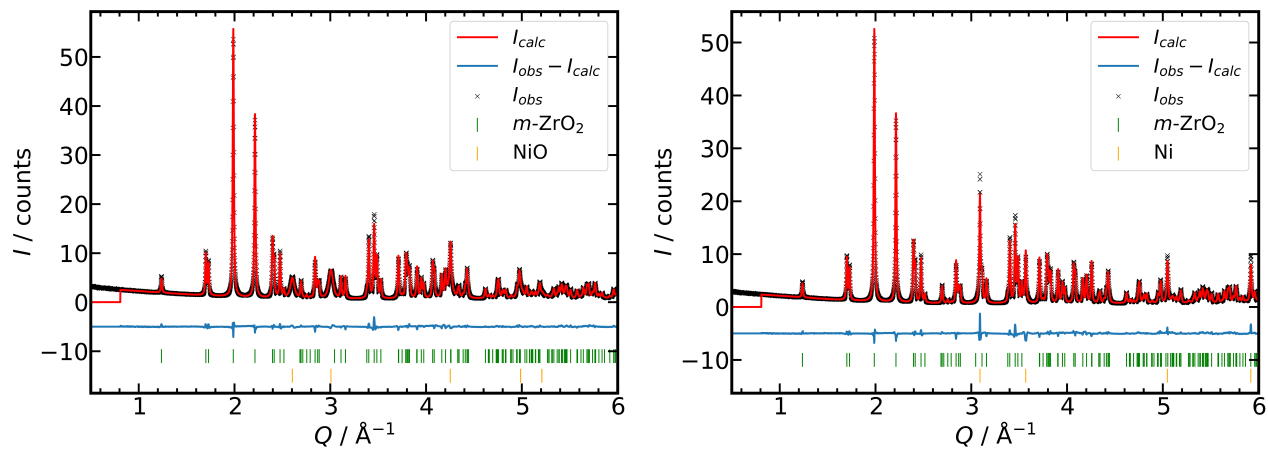


Figure S 37 Rietveld refinements of the initial state before (left) and after (right) *operando* SPXRD experiments of NZ800.

Table S 12 Selected Rietveld refinement results for the NZ800 catalysts in the initial state and after *operando* SPXR.

	NZ800 initial		NZ800 after	
phase	m-ZrO ₂	NiO	m-ZrO ₂	Ni
space group	<i>P</i> 2 ₁ / <i>c</i>	<i>R</i> ̄3 <i>m</i>	<i>P</i> 2 ₁ / <i>c</i>	<i>F</i> ̄ <i>m</i> 3 <i>m</i>
<i>R</i> _{exp} / %	50.00		52.34	
<i>R</i> _{wp} / %	4.26		5.18	
<i>R</i> _p / %	3.19		3.72	
<i>GOF</i> / %	0.09		0.10	
<i>ω</i> / wt.%	80.1(3)	19.9(3)	85.25(11)	14.75(11)
<i>L</i> _{vol} / nm	36.1(9)	9.91(16)	35.0(7)	28.9(4)
<i>η</i> /	0.00043(2)	0.00169(6)	0.00034(2)	0.00000(10)
<i>a</i> / Å	5.14135(10)	2.954(16)	5.14115(9)	3.52075(5)
<i>b</i> / Å	5.20473(11)	-	5.20342(10)	-
<i>c</i> / Å	5.30929(11)	7.24(8)	5.31025(10)	-
<i>β</i> / °	99.2067(10)	-	99.2056(10)	-
	Zr1	Ni1	Zr1	Ni 1
<i>x</i>	0.27508(12)	0	0.27532(12)	0
<i>y</i>	0.03962(10)	0	0.03989(10)	0
<i>z</i>	0.20880(12)	0	0.20874(12)	0
<i>B</i> _{iso} / Å ²	0.00(2)	0.00(6)	0.00(3)	0.00(4)
<i>occ</i>	1	1	1	1
	O1	O1	O1	
<i>x</i>	0.0754(8)	0	0.0733(8)	
<i>y</i>	0.3315(7)	0	0.3309(7)	
<i>z</i>	0.3460(7)	1/2	0.3461(7)	
<i>B</i> _{iso} / Å ²	0.26(10)	0.30(13)	0.09(10)	
<i>occ</i>	1	1	1	
	O2	O2		
<i>x</i>	0.4505(8)		0.4504(8)	
<i>y</i>	0.7594(7)		0.7584(7)	
<i>z</i>	0.4777(10)		0.4750(11)	
<i>B</i> _{iso} / Å ²	0.89(11)		0.57(11)	
<i>occ</i>	1		1	

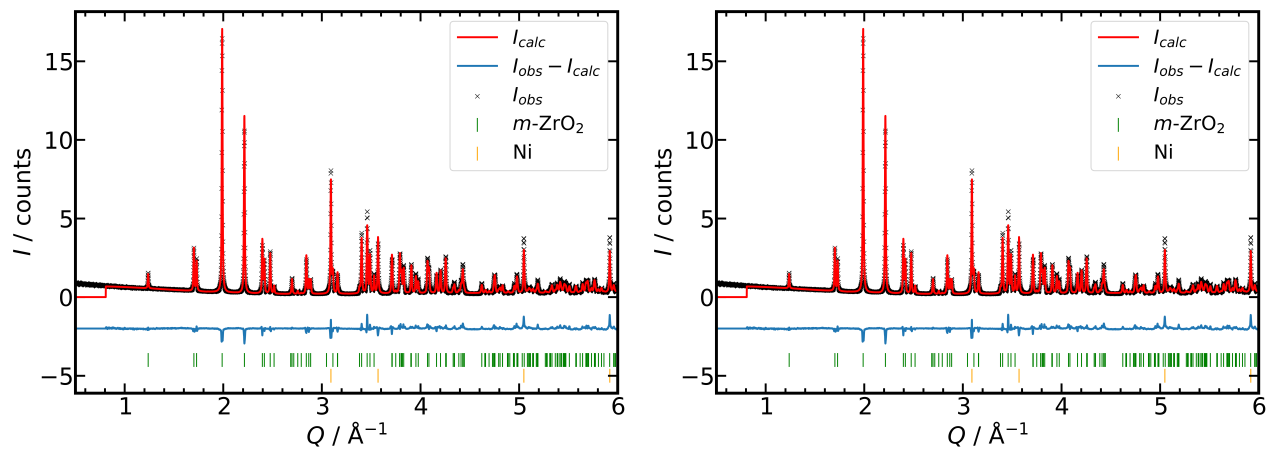


Figure S 38 Rietveld refinements of the initial state before (left) and after (right) *operando* SPXRD experiments of NZ1000.

Table S 13 Selected Rietveld refinement results for the NZ1000 catalysts in the initial state and after *operando* SPXRD.

	NZ1000 initial		NZ1000 after	
phase	m-ZrO ₂	NiO	m-ZrO ₂	Ni
space group	<i>P</i> 2 ₁ / <i>c</i>	<i>R</i> ̄3 <i>m</i>	<i>P</i> 2 ₁ / <i>c</i>	<i>F</i> ̄ <i>m</i> 3 <i>m</i>
<i>R</i> _{exp} / %	35.72		102.44	
<i>R</i> _{wp} / %	8.85		9.10	
<i>R</i> _p / %	7.08		7.14	
<i>GOF</i> / %	0.25		0.09	
<i>ω</i> / wt.%	79.8(3)	20.2(3)	84.9(2)	15.1(2)
<i>L</i> _{vol} / nm	60.0(6)	8.9(2)	67.1(10)	53.4(15)
<i>η</i> /	0.000462(7)	0.00101(19)	0.000475(9)	0.00000(8)
<i>a</i> / Å	5.14031(11)	2.955(4)	5.14034(14)	3.51991(7)
<i>b</i> / Å	5.20115(12)	-	5.20045(15)	-
<i>c</i> / Å	5.31061(13)	7.23(2)	5.31118(16)	-
<i>β</i> / °	99.1824(12)	-	99.1816(16)	-
	Zr1	Ni1	Zr1	Ni 1
<i>x</i>	0.27520(19)	0	0.2754(3)	0
<i>y</i>	0.03921(15)	0	0.0395(2)	0
<i>z</i>	0.20866(17)	0	0.2084(2)	0
<i>B</i> _{iso} / Å ²	0.00(3)	0.00(10)	0.00(4)	0.00(7)
<i>occ</i>	1	1	1	1
	O1	O1	O1	
<i>x</i>	0.0743(11)	0	0.0718(16)	
<i>y</i>	0.3343(11)	0	0.3341(15)	
<i>z</i>	0.3478(10)	1/2	0.3477(14)	
<i>B</i> _{iso} / Å ²	0.00(16)	0.0(2)	0.0(2)	
<i>occ</i>	1	1	1	
	O2		O2	
<i>x</i>	0.4514(12)		0.4514(16)	
<i>y</i>	0.7590(9)		0.7596(13)	
<i>z</i>	0.4819(14)		0.477(2)	
<i>B</i> _{iso} / Å ²	0.00(16)		0.0(2)	
<i>occ</i>	1		1	

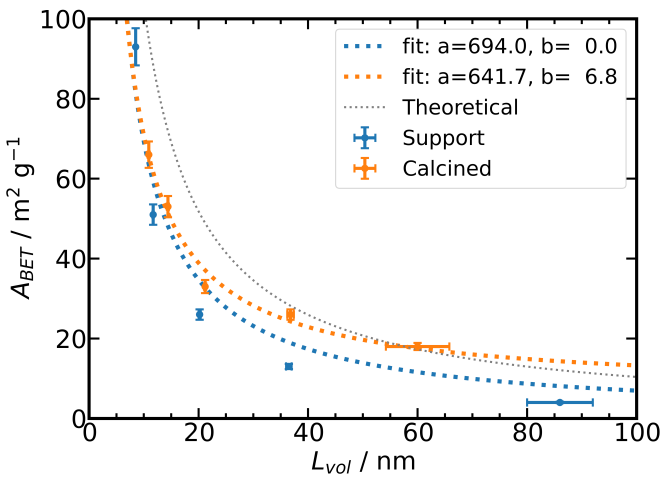


Figure S 39 Correlation of A_{BET} and L_{vol} of the ZrO_2 phase for the pure supports before Ni deposition (blue) and the as-prepared calcined catalysts (orange).

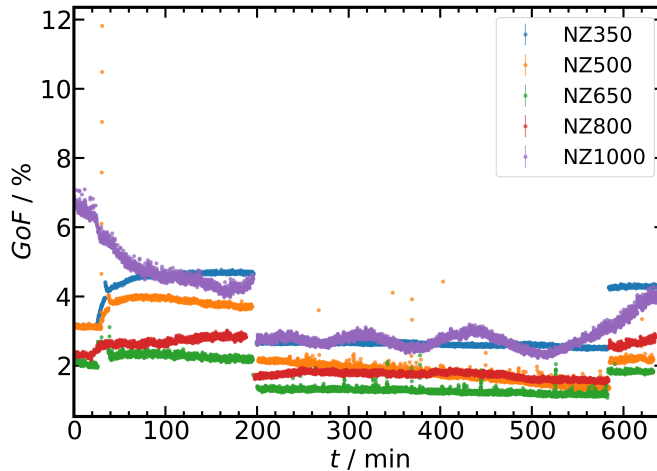


Figure S 40 GOF obtained for the sequential Rietveld refinements. Steps origin in different acquisition time of the SPXRD during activation and final cool-down (9 s) as well as reaction and thermal deactivation cycles (3 s).

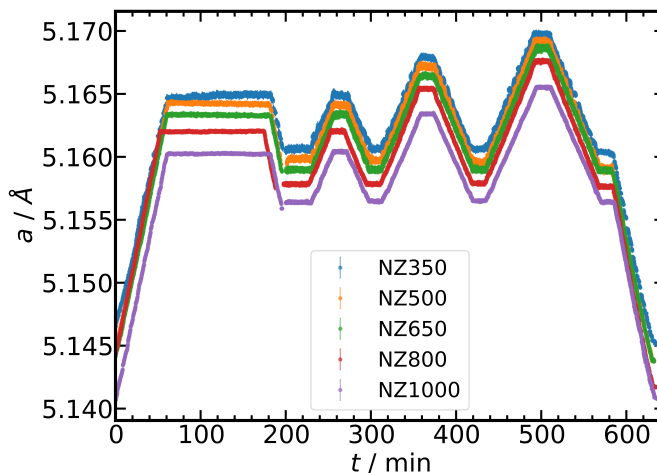


Figure S 41 ZrO_2 lattice parameter a obtained from the sequential Rietveld refinements.

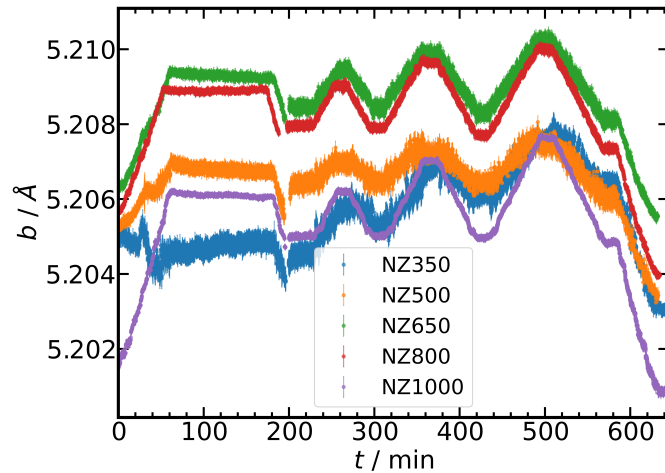


Figure S 42 ZrO_2 lattice parameter b obtained from the sequential Rietveld refinements.

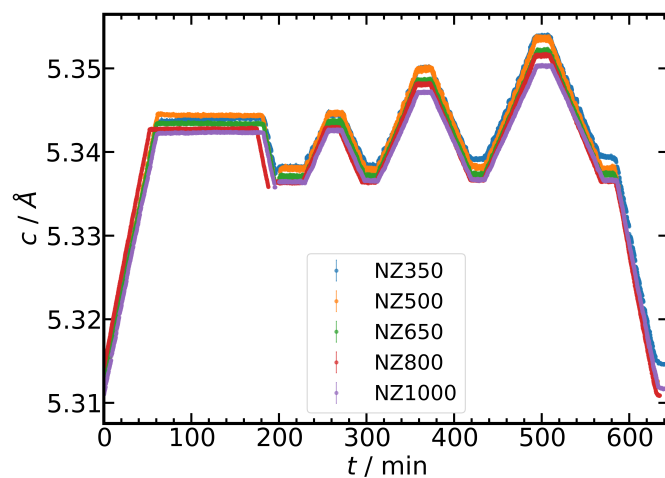


Figure S 43 ZrO_2 lattice parameter c obtained from the sequential Rietveld refinements.

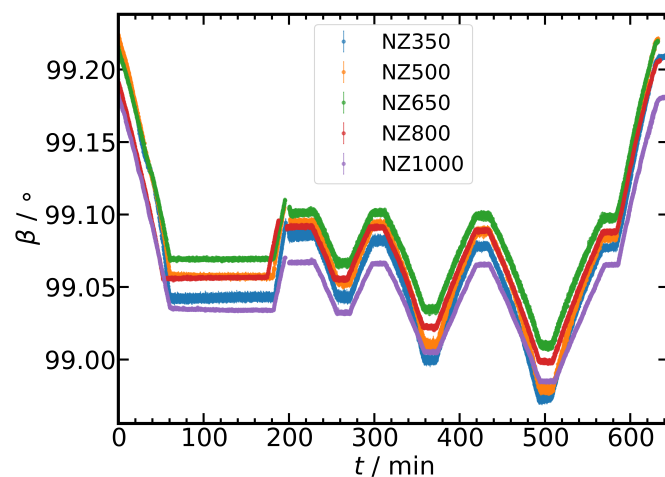


Figure S 44 ZrO_2 lattice parameter β obtained from the sequential Rietveld refinements.

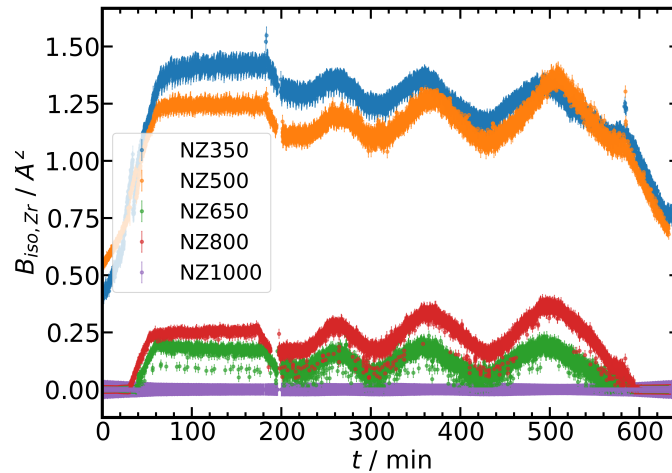


Figure S 45 ZrO_2 phase B_{iso} for Zr obtained from the sequential Rietveld refinements.

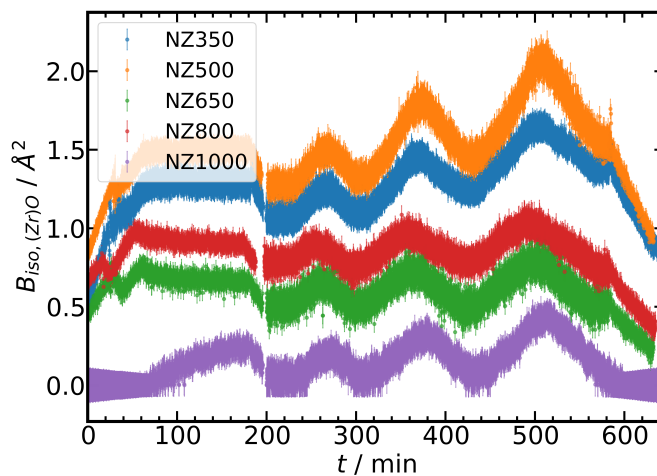


Figure S 46 ZrO_2 phase B_{iso} for O obtained from the sequential Rietveld refinements.

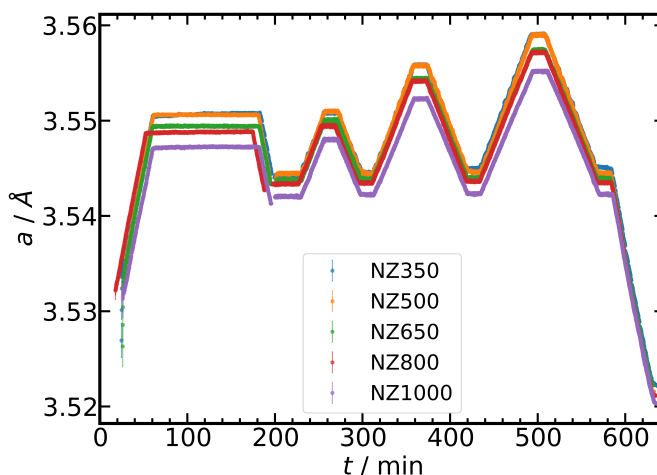


Figure S 47 Ni lattice parameter a obtained from the sequential Rietveld refinements.

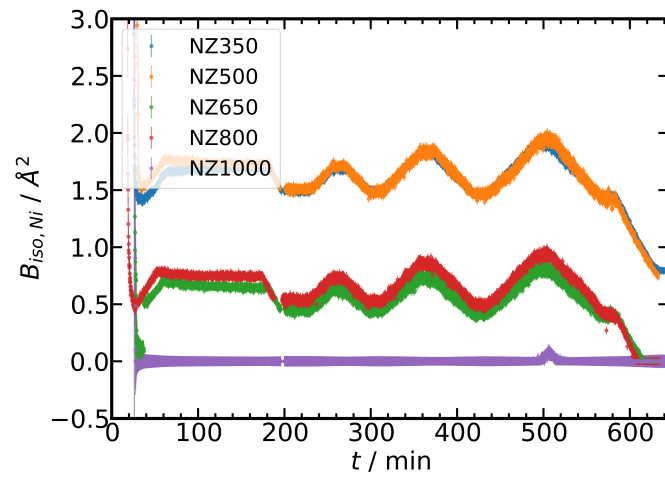


Figure S 48 Ni phase B_{iso} for Ni obtained from the sequential Rietveld refinements.

References

- [1] B. Mutz, M. Belimov, W. Wang, P. Sprenger, M. A. Serrer, D. Wang, P. Pfeifer, W. Kleist and J.-D. Grunwaldt, *ACS Catal.*, 2017, **7**, 6802–6814.
- [2] A. Borodziński and M. Bonarowska, *Langmuir*, 1997, **13**, 5613–5620.
- [3] *Lehrbuch der anorganischen Chemie*, 2007.
- [4] H. M. Rietveld, *Acta Crystallogr.*, 1967, **22**, 151–152.
- [5] H. M. Rietveld, *J. Appl. Crystallogr.*, 1969, **2**, 65–71.
- [6] *DIFFRAC.SUITE TOPAS - XRD Software Bruker*, 2020, <https://www.bruker.com/de/products/x-ray-diffraction-and-elemental-analysis/x-ray-diffraction/xrd-software/topas.html>.
- [7] D. Balzar, *International union of crystallography monographs on crystallography*, 1999, **10**, 94–126.
- [8] R. Delhez, T. H. De Keijser, J. Langford, D. Louër, E. Mittemeijer and E. Sonneveld, *The Rietveld Method (IUCR Book Series)*, 1993, 132.
- [9] V. Honkimäki and P. Surotti, *Defect and Microstructure Analysis by Diffraction (IUCR Book Series)*, 1999.
- [10] D. K. Smith and W. Newkirk, *Acta Crystallogr.*, 1965, **18**, 983–991.
- [11] *J. Mater. Sci.*, 1995, **30**, 1621–1625.
- [12] D. Rodic, V. Spasojevic, V. Kusigerski, R. Tellgren and H. Rundlof, *Phys. Status Solidi B Basic Res.*, 2000, **218**, 527–536.
- [13] J. Rouquette, J. Haines, G. Fraysse, A. Al-Zein, V. Bornand, M. Pintard, P. Papet, S. Hull and F. Gorelli, *Inorg. Chem.*, 2008, **47**, 9898–9904.
- [14] <http://topas.dur.ac.uk/topaswiki/doku.php?id=topas>, accessed on 18/10/2021.